Chalcogenopyrylium Compounds as Modulators of the ATP-Binding Cassette Transporters P-Glycoprotein (P-gp/*ABCB1*) and Multidrug Resistance Protein 1 (MRP1/*ABCC1*)

Sean P. Ebert,[†] Bryan Wetzel,[†] Robert L. Myette,[‡] Gwenaëlle Conseil,[‡] Susan P. C. Cole,[‡] Geri A. Sawada,[§] Tip W. Loo,[∥] M. Claire Bartlett,[∥] David M. Clarke,[∥] and Michael R. Detty*,[†]

[†]Department of Chemistry, University at Buffalo, The State University of New York, Buffalo, New York 14260-3000, United States
[‡]Department of Pathology & Molecular Medicine, Division of Cancer Biology & Genetics, Queen's University, Kingston, Ontario K7L 3N6, Canada
[§]Drug Disposition, Eli Lilly and Company, Indianapolis, Indiana 46285, United States
[∥]Department of Medicine and Department of Biochemistry, University of Toronto, Toronto, Ontario M5S 1A8, Canada

ABSTRACT: Twenty-seven chalcogenopyrylium derivatives varying in the heteroatom of the pyrylium core and substituents at the 2-, 4-, and 6-positions were examined for their effect on human MRP1-mediated uptake of tritiated estradiol glucuronide into inside-out membrane vesicles, their affinity for and ability to stimulate the ATPase activity of purified human P-glycoprotein (P-gp)-His$_{10}$, and their ability to promote uptake of calcein AM and vinblastine in multidrug-resistant cells. Differences in their effects on MRP1 and P-gp activity were noted, and a second set of thiopyrylium compounds with systematic substituent changes was examined to refine these differences further. Derivatives with *tert*-butyl substituents in the 2- and 6-positions had the lowest inhibitory activity toward both transporters. Derivatives with thioamide functionality in the 4-position were more active against MRP1 than derivatives with amide functionality. Conversely, derivatives with amide functionality in the 4-position were more active in P-gp than derivatives with thioamide functionality.
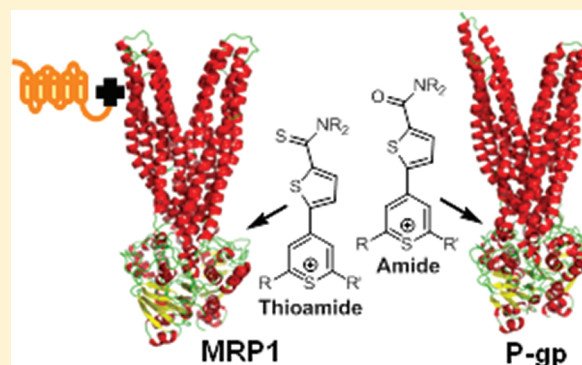
INTRODUCTION

The effective treatment of cancer with chemotherapeutic agents is often limited by the emergence of multidrug resistance (MDR) in the malignant cells. While drug resistance is a consequence of a variety of mechanisms, efflux proteins that are members of the ATP-binding cassette (ABC) superfamily of membrane proteins are most commonly associated with the emergence of MDR.[1,2] Within this family of 48 proteins, three transporters [P-glycoprotein or P-gp (encoded by *ABCB1*), multidrug resistance protein 1 or MRP1 (encoded by *ABCC1*), and breast cancer resistance protein or BCRP (encoded by *ABCG2*)] are the most important in drug-resistant tumors.[2−5] The onset of human P-gp expression and drug resistance can be quite rapid, with elevated expression of the gene for P-gp (*ABCB1*) being observed within an hour of treatment.[6]

The core structure of functional ABC transporters consists of two nucleotide binding domains (NBDs) that bind and hydrolyze ATP and two transmembrane domains (TMDs). Transporters encoded as a single polypeptide, such as P-gp, contain two NBDs and two TMDs in a single protein, while half transporters, such as BCRP, contain only one TMD and one NBD and must dimerize to carry out their function.[6]

P-gp was the first efflux protein identified and associated with multidrug resistance in cancer chemotherapy.[1,2,7,8] A recent crystal structure (3.8 Å resolution) of cys-less mouse P-gp in the absence of nucleotide shows an internal cavity of ∼6000 Å^3 with the NBDs separated by ∼30 Å and portals to both the cytoplasm and inner leaflet of the membrane.[9] Discrete drug-binding pockets were also observed in crystals of drug-P-gp complexes.[9] P-gp is able to transport a diverse array of anticancer drugs including anthracyclines, *Vinca* alkaloids, taxanes, epipodophyllotoxins, and agents such as mitomycin C and trimetrexate.[10−12] Many approaches to the development of inhibitors/modulators of P-gp have been examined,[7,8] yet there are currently no approved reversal agents available in the clinic.[5,13,14]

The ABCC subfamily of ABC proteins includes nine MRP-related transporters.[15−17] In addition to two NBDs and two TMDs, MRP1 and MRP2, 3, 6, and 7 have a third TMD while MRP4, 5, 8, and 9 lack the third TMD and, thus, are structurally more similar to P-gp. While there are no high-resolution structures of the intact MRP1 protein, low resolution studies (∼22 Å) suggest it forms dimers with each monomer containing a central pore of ∼80 × 100 Å^2.[18] MRP1 has 15% amino acid sequence homology with P-gp and, like P-gp,

Chart 1. Structures of Chalcogenopyrylium Compounds Evaluated As Modulators of MRP1 and P-gp
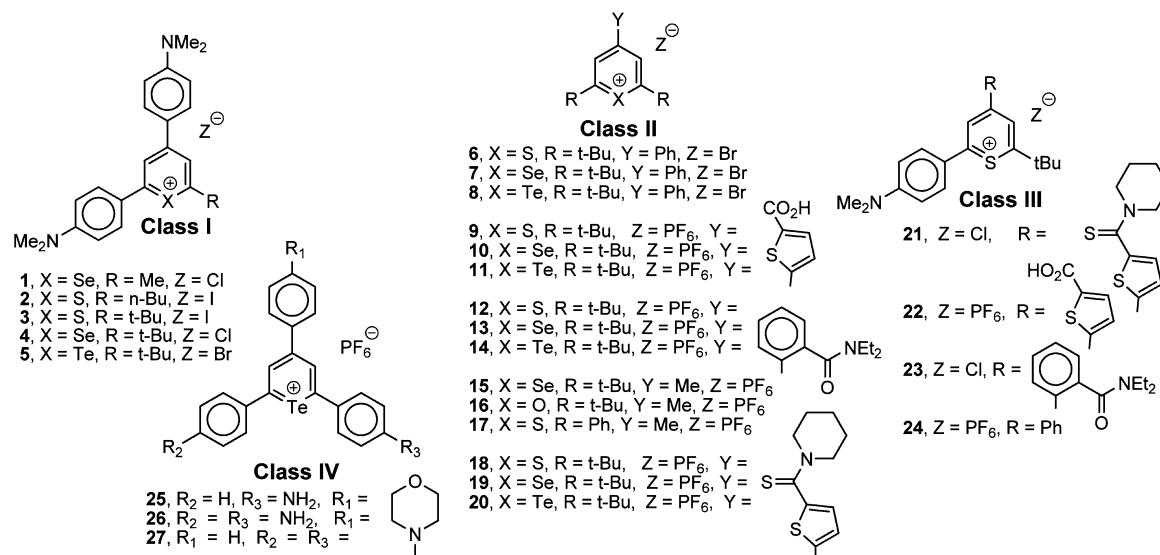
transports a variety of different classes of compounds[19] including anticancer compounds such as the anthracyclines and the *Vinca* alkaloids (in a GSH-dependent manner) as well as methotrexate.[16,17] In addition, and unlike P-gp, MRP1 is a very efficient transporter of a vast array of conjugated organic anions and mediates the physiological efflux of the pro-inflammatory leukotriene C4 from mast cells.[17] Relatively few MRP1-specific inhibitors have been described, and none of these have yet been tested in humans.[16,17]

To understand the ABC drug transporters, we need to study the similarities and differences between transporters with a different number of TMDs. In particular, differences in ATP hydrolysis at the two ATP-binding sites may be critical to the design of specific inhibitors of individual ABC drug tranporters. The two sites in P-gp are similar,[19,20] while the two sites in MRP1 are different.[21] In some situations, it would be useful to inhibit only one transporter to prevent side effects. For example, if one wanted enhanced delivery to the brain then it would be useful only to inhibit P-gp activity. In other cases, such as overexpression of both P-gp and MRP1 in a cancer cell, it would be useful to inhibit both pumps with a single compound.

Chalcogenorhodamine/rosamine derivatives[23−25] and chalco-genopyrylium derivatives[26] are lipophilic cations that bind to P-gp and can act as stimulators or inhibitors of the transporter's ATPase activity and can act as inhibitors of the transporter's ability to efflux small molecules from the cell. With respect to inhibition of P-gp, submicromolar IC_{50}'s for inhibition of verapamil(**VER**)-induced stimulation of ATPase activity have been observed with several chalcogenorhodamine[25] and chalcogenopyrylium compounds.[26] The two classes of modulators share some structural similarities and, in both cases, have slow rates of active transport in MDCKII-MDR1 cells.[25,26] Reactivity with other ABC transporters has not yet been examined. With the chalcogenopyrylium scaffold, myriad analogues are readily prepared with variation at the 2-, 4-, and 6-positions around the ring and at the heteroatom in the ring. The chalcogenopyrylium compounds are model systems that allow exploration of structure−activity space while readily accessible synthetically. Furthermore, chalcogenopyrylium compounds have been successfully utilized as photosensitizers in vitro and in vivo in the photodynamic therapy of cancer

cells/tumors[27] and structurally related chalcogenorhodamine/rosamine derivatives have targeted multidrug-resistant cells in vitro.[28,29] Chalcogenopyrylium compounds with high specificity for one or multiple ABC transporters may be quite useful in vivo as photosensitizers for multidrug-resistant tumors via irreversible photodynamic damage to the efflux pumps.

Herein, we evaluate the 27 chalcogenopyrylium dyes shown in Chart 1 as modulators/inhibitors of MRP1 and P-gp in order to compare and contrast reactivity patterns with the two structurally and functionally distinct transporters. Compounds **3** and **4** in Chart 1 have shown activity as inhibitors of P-gp (IC_{50} ∼5 μM) by increasing calcein AM (CAM) uptake in MDCKII-MDR1 cells,[26] which suggested that the compounds of Chart 1 would provide an initial comparison of the SAR for the two transporters. On the basis of the initial screen of the compounds in Chart 1 with MRP1 and P-gp, the compounds **28−32** shown in Chart 2 were synthesized and the individual

Chart 2. Structures of Chalcogenopyrylium Compounds Evaluated As Modulators of MRP1 and P-gp
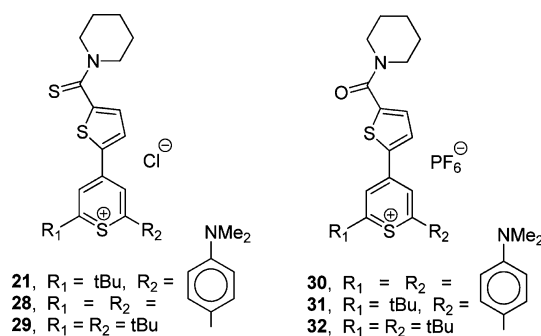
compounds, as well as compound **21** from Chart 1, were evaluated as inhibitors of both MRP1 and P-gp in order to examine the effect of small structural variations on reactivity with the two transporters.

■ CHEMISTRY RESULTS AND DISCUSSION

Synthesis of Chalcogenopyrylium Analogues. The chalcogenopyrylium compounds evaluated in this study can

Scheme 1. Synthesis of Class II Chalcogenopyrylium Derivatives 6−11
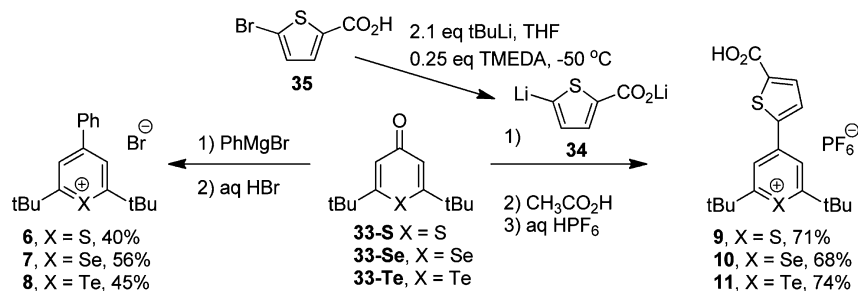
Scheme 2. Synthesis of Class II Chalcogenopyrylium Derivatives 12−14 and 18−20
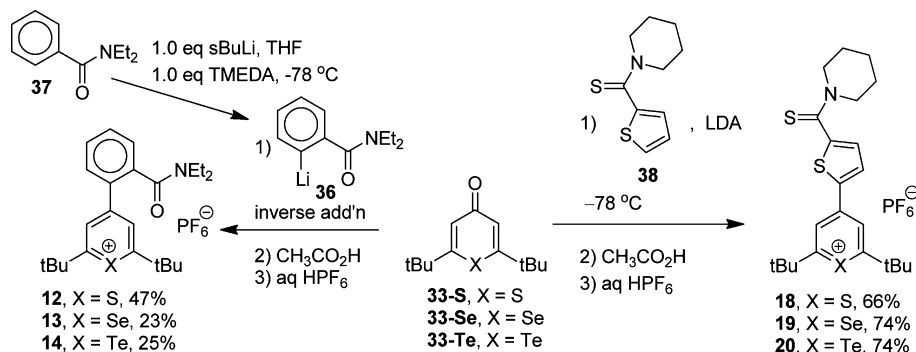
be broadly grouped into four classes as shown in Chart 1. The class I compounds all contain 4-dimethylaminophenyl substituents at the 2- and 4-positions of the chalcogenopyrylium ring. Compounds **1−5** were selected from a library of chalcogenopyrylium dyes that we have prepared as photodynamic antimicrobial agents and were prepared by literature methods.[30,31] The class II compounds are characterized by two identical substituents at the 2- and 6-positions (*tert*-butyl groups for **6−16** and **18−20** and phenyl groups for **17**). Among the class II chalcogenopyrylium compounds, compounds **15−17** are intermediates for the preparation of other dyes and were prepared by literature methods.[32,33] The class III chalcogenopyrylium compounds are characterized by a 2-*tert*-butyl substituent and a 6-(4-dimethylaminophenyl) substituent on the thiopyrylium core. The class IV compounds **25−27** were selected from a library of AA1-related[34] photosensitizers for photodynamic therapy (PDT) and also were prepared by literature methods.[35]

The class II compounds **6−11** were prepared as shown in Scheme 1. The addition of excess PhMgBr to 2,6-di-*tert*-butylchalcogenopyran-4-ones (**33**)[36] followed by the addition of aqueous HBr gave the 4-phenylchalcogenopyrylium bromides **6−8** in 40−56% isolated yield. Compounds **9−11** were prepared by the addition of lithium 5-lithiothiophene-5-carboxylate (**34**) to chalcogenopyranones **33**. Dianion **34** was prepared from 2-carboxy-5-bromothiophene (**35**) using only 2.1 equiv of *tert*-BuLi (1 equiv to deprotonate the acid and only 1 equiv for the metal−halogen exchange) in the presence of 0.25 equiv of TMEDA.[37] Elimination of HBr from the *tert*-BuBr generated in the metal−halogen exchange was not competitive kinetically in these reactions.[38] The addition of **34** to chalcogenopyranones **33** gave chalcogenopyrylium compounds **9−11** in 68−74% isolated yield following workup with aqueous HPF6.

Chalcogenopyrylium derivatives **12−14** and **18−20** were prepared as shown in Scheme 2. The *N,N*-diethylbenzamide-

containing derivatives **12−14** were prepared by the addition of chalcogenopyranones **33** to *N,N*-diethyl 2-lithiobenzamide (**36**).[25,39] Anion **36** was prepared by the deprotonation of *N,N*-diethyl benzamide (**37**) with *sec*-BuLi in the presence of 1.0 equiv of TMEDA at −78 °C. Chalcogenopyrylium compounds **12−14** were isolated in 23−47% isolated yield following workup with aqueous HPF6. Yields were much poorer with the inverse addition of anion **36** to chalcogenopyranones **33**. Thioamide **38** was prepared in 81% isolated yield from thiophene-2-carboxaldehyde under Willgerodt−Kindler conditions with elemental sulfur and piperidine.[25] Deprotonation of **38** with lithium diisopropylamide (LDA) occurred from the sterically least hindered 5-position to give *N*-piperidyl 5-lithio-2-thiocarboxythiophene (**39**), which was added to chalcogenpyranones **33** to give chalcogenopyrylium compounds **18−20** in 66−74% isolated yield following workup with aqueous HPF6. Unlike the tertiary amide group,[39] which is highly directing as in the preparation of **36**, the thioamide functionality does not direct lithiation in thiophenes. Only the more acidic α-proton was removed, and none of the corresponding 2,3-disubstituted thiophenes were detected in the product mixtures.

The class III chalcogenopyrylium compounds **21−24** were prepared as shown in Scheme 3. The addition of PhMgBr, anion **36**, or dianion **37** to 2-*tert*-butyl-6-(4-dimethylaminophenyl)-thiopyran-4-one (**40**)[30] gave thiopyrylium derivatives **22−24** in 45−87% isolated yields. Addition of the anion **39** from thioamide **38** and LDA to thiopyranone **40** followed by workup with aqueous HPF6 gave the PF6 salt of **21** (compound **41** in Scheme 4), which was converted to the chloride salt **21** with an ion-exchange resin.

As described below, thiopyrylium analogue **21** was an effective modulator/inhibitor of MRP1 and P-gp. We prepared a series of five additional compounds as shown in Scheme 4 that were related in structure to **21** by varying all combinations

Scheme 3. Synthesis of Class III thiopyrylium derivatives 21−24
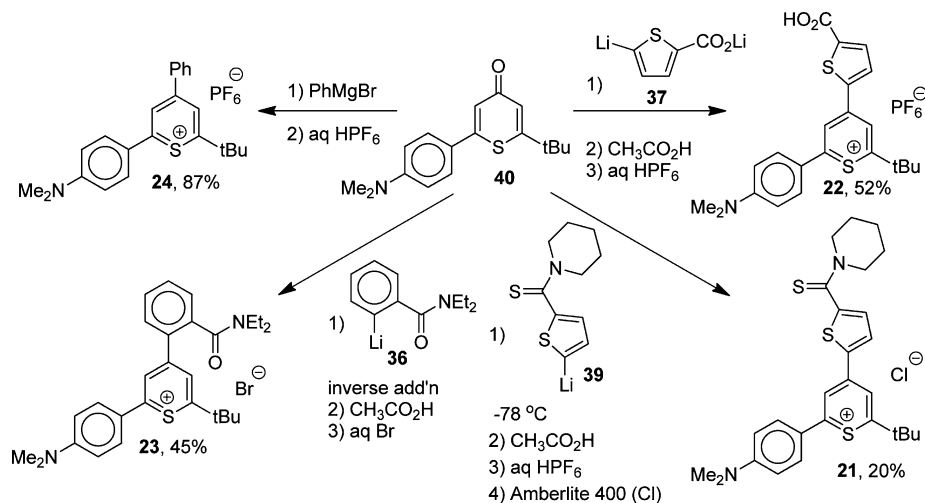
Scheme 4. Synthesis of the Amide and Thioamide Thiopyrylium Derivatives 21 and 28−32
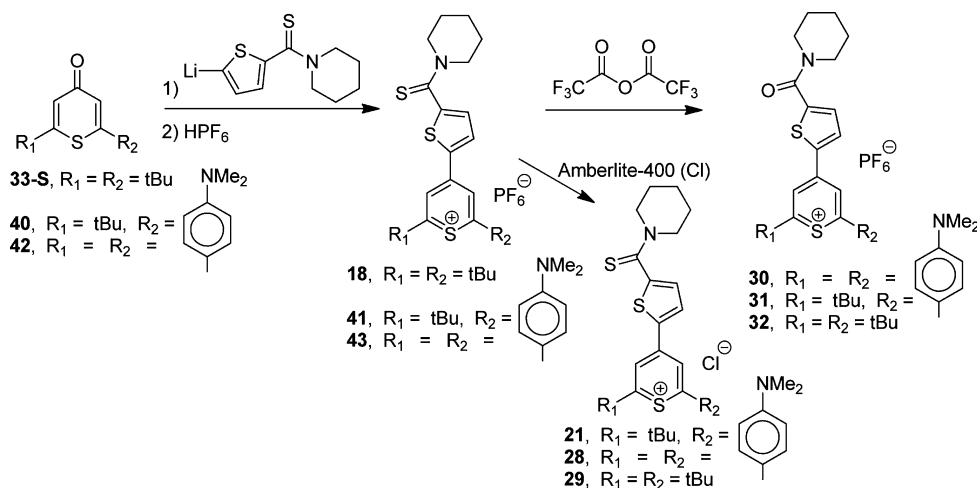
of *tert*-butyl and 4-dimethylaminophenyl substituents at the 2- and 6-positions in the thiopyrylium core and varying amide and thioamide functionality at the 4-position. The addition of anion **39** to thiopyranones **33-S**, **40**, and **42**[40] followed by workup with aqueous HPF$_6$ gave thiopyrylium compounds **18**, **41**, and **43**, which were converted to the chloride salts **29**, **21**, and **28**, respectively, with a chloride exchange resin. Thiopyrylium thioamides **18**, **41**, and **43** were converted to the thiopyrylium amide derivatives **30−32** with trifluoroacetic anhydride.[25] The amide compounds **30−32** were evaluated as the hexafluorophosphate salts because the corresponding chloride salts were hygroscopic and difficult to store. These six compounds were evaluated as modulators of both MRP1 and P-gp to examine the impact of small structural modifications on reactivity patterns in the two transporters.

***n*-Octanol/Water Partition Coefficients.** Experimental values of the *n*-octanol/water (PBS) partition coefficient (log *P*) were measured using the "shake flask" method.[41] Saturated *n*-octanol solutions of chalcogenopyrylium compounds **21** and **28−32** were shaken with an equal volume of phosphate buffered saline (PBS) at pH 7.4, and the concentrations in the two layers were determined spectrophotometrically. Experimental values of log *P* are compiled in Table 2 for these compounds.

■ BIOLOGICAL RESULTS

Effect of Chalcogenopyrylium Compounds 1−27 on MRP1-Mediated Vesicular Uptake of [³H]E$_2$17βG. To determine whether the 27 chalcogenopyrylium dyes of Chart 1 could modulate MRP1 transport activity, their effect on MRP1-mediated uptake of tritiated estradiol glucuronide ([³H]-E$_2$17βG) into inside-out membrane vesicles was assessed.[42] A stably transfected HEK-MRP1 cell line was used as a source for membrane vesicles.[43] Following immunoblot analysis to confirm the expression of MRP1 (Figure 1), the vesicles were initially tested for their [³H]E$_2$17βG uptake activity to assess the integrity of the vesicles as reflected by their baseline transport levels.

Having confirmed the transport competence of the MRP1-enriched membrane vesicles, the 27 chalcogenopyrylium compounds were screened at a single concentration of 30 μM, with the exception of **1**, **7**, **9**, **17**, and **26**, which were tested at 1 μM, and chalcogenopyrylium compounds **2**, **10**, **11** and **20**, which were tested at 5 μM. Testing these latter compounds at a concentration <30 μM was necessary because of either insufficient solubility and/or because they generated an unacceptably high background which interfered with accurate scintillation counting in the transport assay.
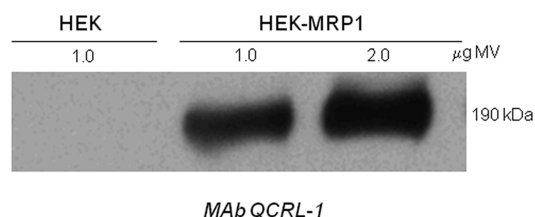
Figure 1. Expression of human MRP1 protein in membrane vesicles. Immunoblots of membrane vesicles (MV) prepared from transfected (1.0 and 2.0 μg of protein) and untransfected (1.0 μg of protein) HEK293T cells are shown. mAb QCRL-1 was used to detect MRP1. HEK refers to control membrane vesicles prepared from untransfected cells.

As summarized in Table 1, the modulatory effects of the 27 chalcogenopyrylium compounds on MRP1-mediated uptake of [^{3}H]E$_2$17βG varied significantly. Ten of 27 (**2–5, 18, 19, 21, 22, 25,** and **27**) inhibited MRP1-mediated uptake by 70–96%. Nine of the remaining 17 (**1, 7, 9–11, 15–17,** and **26**) inhibited [^{3}H]E$_2$17βG uptake by less than 30%. Inhibition by the other eight chalcogenopyrylium compounds (**6, 8, 12–14,** **20, 23,** and **24**) ranged from 30 to 50%. However, it should be noted that **1, 7, 9, 17,** and **26** could only be tested at a maximum concentration of 1 μM, while chalcogenopyrylium compounds **2, 10, 11,** and **20** could only be tested at a maximum concentration of 5 μM. Therefore, the efficacy of these latter nine chalcogenopyrylium compounds (six of which were from class II) may be underestimated.

Four of five class I chalcogenopyrylium compounds (**2–5**) were effective inhibitors of MRP1-mediated [^{3}H]E$_2$17βG uptake, with mean inhibition values ranging from 70 to 96% when tested at 30 μM (Table 1). The remaining compound **1** inhibited uptake of [^{3}H]E$_2$17βG by only 15% at 1 μM.

In contrast to the class I compounds, the 15 class II chalcogenopyrylium compounds **6–20** were relatively ineffective inhibitors of MRP1 transport activity. Only **18** and **19** inhibited [^{3}H]E$_2$17βG uptake by more than 70% (Table 1) at 71 and 81%, respectively. Inhibition by **20** (the telluropyrylium analogue of **18** and **19**) was 50%. For the remaining 12 class II compounds, inhibition ranged from 0 to 45%. However, for reasons stated earlier, 6 of these 12 were tested at concentrations <30 μM and, thus, their relative efficacy may be underestimated.

Table 1. Effect of Chalcogenopyrylium Compounds 1–27 on Human MRP1-Mediated [^{3}H]E$_2$17βG Uptake, Stimulation of Human P-gp-His$_{10}$ ATPase Activity, and P-gp Inhibition in MDCKII-MDR1 Cells

	MRP1		human P-gp-His$_{10}$		% inhibition (44, LSN 335984)	
compd	conc, μM	% inhibition[a]	V_{max},[b] fold	K_M,[c] μM	5 μM	25 μM
VER			17.9 ± 2.0	24 ± 2.6		
1	1	15 (22, 8)	1.4 ± 0.2	13.2 ± 0.3		
2	5	70 (77, 61)	5.9 ± 0.8	37 ± 12		
3	30	94 (94, 95)	7.2 ± 1.1	13.2 ± 0.7	25[d]	60[d]
4	30	96 (93, 99)	10.1 ± 0.5	31 ± 1	23[d]	67[d]
5	30	96 (94, 98)	8.4 ± 1.0	56 ± 8		
6	30	33 (29, 36)	2.9 ± 0.4	95 ± 6	0	1 ± 2
7	1	0 (0, 0)	1.4 ± 0.2	89 ± 9		
8	30	34 (33,36)	1.5 ± 0.1	86 ± 17		
9	1	8 (1, 15)	3.5 ± 0.7	98 ± 9	0	0
10	5	15 (10, 21)	<1.4	(111 ± 9)		
11	5	24 (15, 34)	<1.4	(162 ± 52)		
12	30	34 (28, 41)	7.9 ± 1.8	52 ± 8	0	0
13	30	31 ± 12	5.9 ± 1.1	17 ± 4		
14	30	45 (53, 38)	6.9 ± 0.8	30 ± 8		
15	30	0 (0, 0)				
16	30	0 (0, 0)				
17	1	0 (0,0)				
18	30	71 (80, 62)	4.4 ± 1.2	52 ± 12	3.6 ± 1.3	27 ± 5
19	30	81 (82, 81)	4.3 ± 1.0	101 ± 10		
20	5	50 ± 2	7.4 ± 1.9	85 ± 13		
21	30	93 (94, 93)	5.2 ± 0.8	24.3 ± 3.8	31 ± 3	74 ± 1
22	30	96 (95, 98)	13.0 ± 3.4	997 ± 100		
23	30	43 (47, 40)	13.5 ± 1.2	13.7 ± 3.2	2 ± 3	13 ± 4
24	30	50 (45, 56)	6.9 ± 0.9	20.0 ± 1.7		
25	30	96 (97, 96)	4.5 ± 0.8	59 ± 10		
26	1	8 (8, 9)	ND[e]	ND[e]		
27	30	89 (91, 87)	4.0 ± 0.3	24.3 ± 4.9		

[a]% inhibition of [^{3}H]E$_2$17βG uptake relative to vehicle control (1% DMSO). Results shown are the mean ± SD of three independent experiments. Where only two experiments were performed, the results of both experiments are shown in parentheses. [b]V_{max} is the ratio of the maximum stimulation in the presence of compound relative to that in the absence of compound (the basal activity). [c]K_M is the apparent Michaelis–Menten constant or the concentration of compound required for half maximal stimulation of P-gp ATPase activity. Values in parentheses are IC$_{50}$ values: the concentration of compound required for 50% inhibition of **VER**-stimulated (400 μM) human P-gp-His$_{10}$ ATPase activity. [d]Values from ref 26. [e]ND, not determined because of spectral interference with the P-gp ATPase activity assay.

Among the class III compounds, **21** and **22** were strong inhibitors of MRP1 transport activity (93% and 96% inhibition of [³H]E₂17βG uptake, respectively) while **23** and **24** displayed more modest inhibition (43% and 50%, respectively). Both class IV compounds that could be used at 30 μM (**25** and **27**) gave strong inhibition of [³H]E₂17βG uptake (96% and 89% inhibition, respectively), while compound **26**, which could be used at only 1 μM, displayed 8% inhibition.

Effect of Chalcogenopyrylium Compounds on Human P-gp-His₁₀ ATPase Activity. The effect of chalcogenopyrylium compounds **1–14** and **18–27** (Chart 1) on P-gp ATPase activity was examined using human P-gp-His₁₀, which was activated with sheep brain phosphatidylethanolamine.[44−46] The apparent Michaelis−Menten constant (K_M) for ATPase-stimulating compounds was determined as well as the drug-induced stimulation of maximal ATPase activity (V_{max}) using human P-gp-His₁₀ (Table 1). P-gp ATPase activity was determined as the release of inorganic phosphate from ATP.[47] A typical ATPase activity vs concentration profile is shown in Figure 2 for chalcogenopyrylium compound **23**, which was the
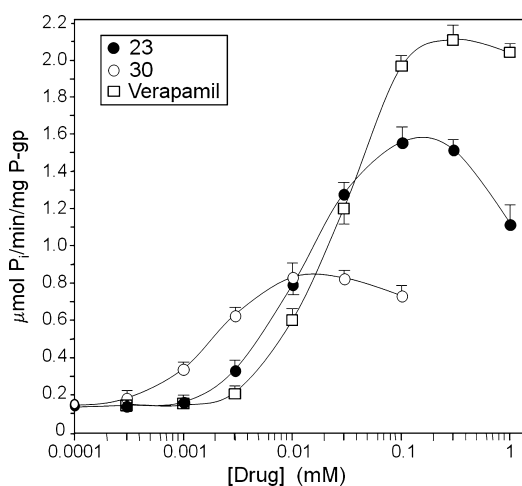
Figure 2. Effect of thiopyrylium compounds on P-gp ATPase activity. His-tagged human P-glycoprotein was expressed in BHK cells, isolated by Ni²⁺-chelate chromatography, and mixed with lipid. P-Glycoprotein ATPase activity was then measured in the presence of various concentrations of thiopyrylium derivatives **23** (filled circles, compound with the largest V_{max}), **30** (open circles, compound with lowest K_M), or **VER** (open squares). Data points represent the mean of triplicate measurements and error bars represent ± one standard deviation.

most effective stimulator of the chalcogenopyrylium analogues examined. Verapamil (**VER**) was included as a control compound because of its well-known ability to stimulate P-gp ATPase activity.[48,49] For compounds **10** and **11**, which only weakly stimulated P-gp ATPase activity, the concentration of compound required for 50% inhibition of **VER**-stimulated (400 μM) ATPase activity (IC_{50}) was determined (Table 1).

Within the class I compounds **1–5**, the stimulation of P-gp ATPase V_{max} ranged from 1.4-fold for compound **1** to 10.1-fold for compound **4** while K_M ranged from 13.2 μM for compounds **1** and **3** to 56 μM for **5**. Among the class II compounds **6–14** and **18–20**, stimulation of V_{max} ranged from <1.4-fold for compounds **10** and **11** to 7.9-fold stimulation for compound **12**; K_M values were higher in this series (52–101 μM), with the exception of compounds **13** and **14**, with K_M values of 17 and 30 μM, respectively. For compounds **9** and **10**, which did not

give sufficient P-gp ATPase stimulation for an accurate determination of K_M, the IC_{50}s for 400 μM **VER**-induced stimulation were 111 and 162 μM, respectively. Among the class III compounds **21–24**, V_{max} values were stimulated 6.2–13.5-fold. Compounds **21**, **23**, and **24** had K_M values between 13.7 and 20.0 μM. In contrast, compound **22** highly stimulated V_{max} (13.1-fold), but its K_M was quite large at 997 μM. Among the class IV compounds, **25** and **27** were assayed and found to be mildly P-gp ATPase stimulating (V_{max} stimulated by 4.5-fold and 4.0-fold, respectively), with corresponding K_M values of 59 and 24.3 μM.

CAM Uptake into MDCKII-MDR1 Transfected Cells. Selected chalcogenopyrylium compounds were also evaluated for their ability to facilitate **CAM** uptake into MDCKII-MDR1 transfected cells, which overexpress P-gp.[50] **CAM** uptake was determined at chalcogenopyrylium concentrations of 5 and 25 μM and P-gp inhibition was measured as a percentage of the inhibition observed with 5 μM (R)-4-[(1a,6,10b)-1,1-dichloro-1,1a,6,10b-tetrahydrodibenzo[a,e]cyclopropa[c]cyclohepten-6-yl]-[(5-quinolinyloxy)methyl]-1-piperazineethanol (**44**, LSN 335984, IC_{50} = 0.4 μM), which completely inhibits P-gp (Chart 3).[14] Compound **44** is structurally related to the P-gp-

Chart 3. Structures of LSN 335984 (44) and LSN 335979 (45)
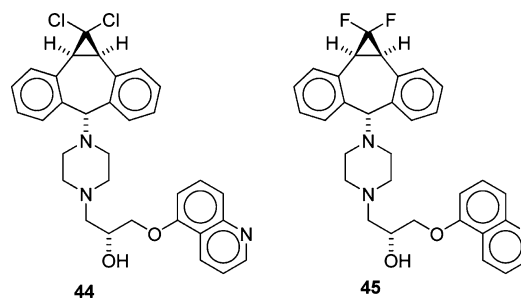
specific inhibitor (R)-4-[(1a,6,10b)-1,1-difluoro-1,1a,6,10b-tetrahydrodibenzo[a,e]cyclopropa[c]cyclohepten-6-yl]-[(5-quin-olinyloxy)methyl]-1-piperazineethanol (**45**, LSN 335979 or zosuquidar).[14,51] The **CAM** fluorescence observed with the chalcogenopyrylium compounds is reported as a percentage of the **CAM** fluorescence observed with 5 μM **44** (100% inhibition). The percentage inhibition at the two chalcogeno-pyrylium concentrations is summarized in Table 1 for compounds **3**, **4**, **6**, **9**, **12**, **18**, **21**, and **23**. Compounds **3** and **4** showed comparable activity in this assay with inhibition of 25 and 23%, respectively, at 5 μM and 60 and 67%, respectively, at 25 μM relative to inhibition by **44**.[26]

Interactions of Amide- and Thioamide-Containing Thiopyrylium Compounds 21 and 28−32 with MRP1 and P-gp. Thiopyrylium compounds **21** and **28−32** (Chart 2) were evaluated at concentrations of 1 and 10 μM for their ability to inhibit MRP1-mediated uptake of [³H]E₂17βG in membrane vesicles (Table 2).[42] At 1 μM, compounds **28** and **30** showed weak inhibition of MRP1-mediated transport (25 and 18%, respectively) while compounds **29**, **31**, and **32** showed no detectable inhibition. At 10 μM, **21** gave 93% inhibition and **28** and **30** were similarly effectively causing 81% and 78% inhibition, respectively; **31** gave 59% inhibition and **29** gave 32% inhibition. Compound **32** was least effective in this series, giving only 11% inhibition at 10 μM.

The effect of the thiopyrylium compounds **21** and **28−32** (Chart 2) on P-gp ATPase activity was also examined using

Table 2. Experimental Values of log P and the Effect of Thiopyrylium Amide and Thioamide Analogues on MRP1-Mediated Transport, P-gp ATPase Activity, and P-gp-Mediated Calcein AM Uptake and Vinblastine Efflux[a]

		MRP1		P-gp			
compd	log P^b	% inhibition 1 μM	% inhibition 10 μM	V_{max},[c] fold	K_{M},[d] μM	IC$_{50}$ CAM uptake, μM	IC$_{50}$ for VIN efflux, μM
21	2.1	36 ± 8	93 (94, 93)	5.2 ± 0.8	24.3 ± 3.8	38.0 ± 1.2	11.5 ± 1.0
28	1.6	25 (24, 25)	81 (84, 79)	5.7 ± 1.0	7.7 ± 0.8	34.0 ± 1.2	6.6 ± 1.0
29	0.7	0 (0, 0)	32 (28, 37)	3.7 ± 0.8	74 ± 12	ND	ND
30	2.1	18 (29, 7)	78 (80, 76)	6.0 ± 1.3	2.2 ± 0.7	18 ± 1	5.9 ± 1.1
31	1.4	0 (0, 0)	59 (60, 59)	6.6 ± 1.4	11.7 ± 3.8	24.0 ± 1.3	ND
32	0.2	0 (0, 0)	11 (13, 10)	5.5 ± 0.9	72 ± 12	ND	ND

[a]Details for methods are provided in Experimental Section. Values shown are means ± one standard deviation when three or more experiments were performed. Where only two experiments were performed, means are shown with individual values of the two experiments in parentheses. [b]Experimental values of log P determined in *n*-octanol and PBS at pH 7.4 using the "shake flask" method. [c]V_{max} is the ratio of the maximum stimulation in the presence of compound relative to that in the absence of compound (the basal activity). [d]K_{M} is the apparent Michaelis–Menten constant and corresponds to the concentration of compound required for half-maximal stimulation of P-gp ATPase activity.

human P-gp-His$_{10}$ activated with sheep brain phosphatidylethanolamine.[44–46] Values for K_{M} and V_{max} are compiled in Table 2. All six compounds weakly stimulated P-gp ATPase activity (3.7- to 6.6-fold) with a 35-fold range in K_{M} values (2.2–74 μM). Thiopyrylium compounds **29** and **32** had the two highest K_{M} values (74 and 72 μM, respectively), compounds **21** and **31** had intermediate K_{M} values (24.3 and 11.7 μM, respectively), and compounds **28** and **30** had the lowest K_{M} values (7.7 and 2.2 μM, respectively). The P-gp ATPase activity vs concentration curve for **30** is shown in Figure 2.

Enhancement of CAM Uptake into MDCKII-MDR1 Cells. Thiopyrylium compounds **21**, **28**, **30**, and **31** were evaluated for their ability to facilitate uptake of **CAM** into MDCKII-MDR1 cells.[50] IC$_{50}$ values for **CAM** uptake (Table 2) were determined by measuring relative fluorescence values obtained after a 20 min incubation with **CAM** at 37 °C. Amide analogues **30** and **31** (IC$_{50}$s of 24 and 18 μM, respectively) were more effective modulators than the corresponding thioamide analogues **21** and **28** (IC$_{50}$s of 38 and 34 μM, respectively). The 2,6-di-*tert*-butylthiopyrylium analogues **29** and **32** were not evaluated in this assay due to their negligible inhibition of P-gp at 5 and 25 μM in the two-concentration **CAM** uptake experiments described above (≤7% inhibition at 25 μM).

Inhibition of Vinblastine Efflux by Thiopyrylium Compounds 21, 28, and 30 in MDCKII-MDR1 Cells. Vinblastine (**VIN**) is a well-known chemotherapeutic agent, and inhibition of **VIN** efflux by the chalcogenopyrylium compounds may be of potential clinical value. [³H]-**VIN** was introduced in an appropriate dilution series with **21**, **28**, or **31** and BSA to the basolateral chamber of a monolayer of MDCKII-MDR1 transfected cells. The appearance of [³H]-**VIN** in the apical chamber was monitored by scintillation counting and gave IC$_{50}$ values of 11.5, 6.6, and 5.9 μM for **21**, **28**, and **30**, respectively. While these IC$_{50}$ values are lower than the corresponding IC$_{50}$ values for **CAM** uptake, the trend observed for **CAM** uptake is continued with the IC$_{50}$ for amide **30** being 2-fold lower than the IC$_{50}$ for the thioamide **21**.

Transport of Thiopyrylium Compounds Across Monolayers of MDCKII-MDR1 Cells. The transport of the thiopyrylium amide and thioamide derivatives **21** and **28–32** was examined in monolayers of MDCKII-MDR1 transfected cells (Table 3).[50] MDCKII-MDR1 monolayers display apical and basolateral polarized membranes and are widely used as a physiological model for studying P-gp mediated drug efflux. In the monolayer, P-gp is asymmetrically distributed, being

Table 3. Effect of Chalcogenopyrylium Analogues 21 and 28−32 on Efflux Activity of MDCKII-MDR1 Cells[a]

compd	P_{AB}, nm s^{-1}	P_{BA}, nm s^{-1}	$P_{BA/AB}$	normalized ratio, $P_{BA/AB}$[b] (∓ inh)	$P_{Passive}$,[c] nm s^{-1}
21	0.3 ± 0.1	320 ± 29	1015	705	2
(+ inh)	1.6 ± 1.3	2.4 ± 0.1	14		
28	1.1 ± 0.1	16 ± 4	15	8	0.6
(+ inh)	0.4 ± 0.1	0.8 ± 0.1	2		
29	1.8 ± 0.2	300 ± 10	167	15	14
(+ inh)	2.3 ± 0.7	25.0 ± 0.2	11		
30	1.7 ± 0.6	620 ± 37	370	79	14
(+ inh)	4.9 ± 2.4	23.0 ± 0.2	4.7		
31	5.6 ± 2.0	22.0 ± 9.0	3.9	4	3.7
(+ inh)	3.9 ± 0.1	3.5 ± 0.1	0.9		
32	3.8 ± 0.2	59.0 ± 3.9	16	10	5.3
(+ inh)	4.2 ± 0.3	6.4 ± 0.1	1.5		

[a]Experiments were run with 5 μM dye and 4.3 mg mL^{-1} BSA. Values of transport in the absorptive (P_{AB}) and secretory (P_{BA}) mode in the absence or presence of inhibitor, the ratio of secretory to absorptive transport ($P_{BA/AB}$) in the absence or presence of inhibitor, the normalized ratio [$P_{BA/AB}$ (no inhibitor)/$P_{BA/AB}$ (with inhibitor)]. Details for methods are provided in the Experimental Section. Values shown are means ± standard deviation. [b]The normalized ratio represents the $P_{BA/AB}$ ratio in the absence of inhibitor divided by the $P_{BA/AB}$ ratio in the presence of inhibitor. [c]$P_{Passive}$ represents the mean of P_{AB} and P_{BA} in the fully inhibited system.

solely present at the apical membrane. To evaluate the role of P-gp in the transport of the compounds of this series, transport was measured in the absorptive (apical to basolateral or AB) and secretory (basolateral to apical or BA) transport direction of the cell monolayer, and then an efflux ratio ($P_{BA/AB}$) was calculated.[52] Addition of bovine serum albumin (BSA) to the buffer was required because a marked fraction of thiopyrylium mass added to the donor equilibrated with the cell monolayer for some of the compounds, and this resulted in gross underestimation of the permeability coefficient.[53] The assay was repeated in the presence of **44** (LSN 335984)[14] to measure transport when P-gp was fully inhibited.

Values of passive transport ($P_{Passive}$) in the presence of inhibitor, transport in the absorptive (P_{AB}) and secretory (P_{BA}) mode in the absence or presence of inhibitor, the ratio of secretory to absorptive transport ($P_{BA/AB}$) in the absence or presence of inhibitor, and the normalized ratio [$P_{BA/AB}$ (no inhibitor)/$P_{BA/AB}$ (with inhibitor)] are compiled in Table 3.

For **21** and **28−32**, the large normalized efflux ratios for $P_{BA/AB}$ (≥ 4) are assumed to be due to efficient P-gp-mediated efflux of the compound and suggest that thiopyrylium compounds **21** and **28−32** are P-gp substrates. Thiopyrylium compound **21** has the highest normalized ratio for $P_{BA/AB}$ (705) and **31**, the lowest (4).

Transport rates in the absorptive direction (P_{AB}) were slow (≤ 5.6 nm s^{-1}) for all six compounds as were rates of $P_{Passive}$ (14 nm s^{-1} for **29** and **30** and ≤ 5.3 nm s^{-1} for **21**, **28**, **31**, and **32**) in fully inhibited systems. In the secretory direction (P_{BA}), the thiopyrylium compounds sorted into two groups. Compounds **28**, **31**, and **32** (1 thioamide, 2 amides) exhibited relatively slow secretory transport rates (P_{BA} 16−59 nm s^{-1}), while compounds **21**, **29**, and **30** (2 thioamides, 1 amide) were transported at a much faster rate (P_{BA} 300−620 nm s^{-1}).

■ DISCUSSION OF BIOLOGICAL RESULTS

The three major transporters [P-gp (encoded by *ABCB1*),[10−12] MRP1 (encoded by *ABCC1*),[16,17,22] and BCRP (encoded by *ABCG2*)[54,55]] show considerable diversity in transportable substrates as well as overlap of transportable substrates. Understanding the differences in the biology and biochemistry of the transporters can lead to mechanistic understanding of why the different transporters prefer different substrates.[56,57] Within the chalcogenopyrylium compounds of this study, differences were noted in their inhibitory activity toward MRP1 and P-gp.

Comparative Interactions of Chalcogenopyrylium Compounds with MRP1 and P-gp. As demonstrated by the results in Tables 1 and 2, chalcogenopyrylium compounds function as inhibitors of MRP1 in membrane vesicles, as modulators (ATPase stimulating as well as inhibiting) of purified human P-gp-His$_{10}$ activated with sheep brain phosphatidylethanolamine, and as P-gp inhibitors in human P-gp expressing MDCKII-MDR1 cells. However, P-gp and MRP1 share only 15% amino acid sequence identity,[19] and one might expect differences in binding as well as differences in modulatory/inhibitory activity within a series of related structures.

The chalcogenopyrylium compounds examined in this study allow some qualitative correlations to be made among the various chalcogenopyrylium classes described here. These results are compiled as a qualitative comparison between MRP1 and P-gp in Table 4. The class I chalcogenopyrylium compounds **2−5** act as strong inhibitors of MRP1 and weaker modulators of P-gp as measured by K_M (Tables 1 and 4) These compounds all share 4-*N,N*-dimethylaminophenyl substituents at the 2- and 4-positions of the chalcogenopyrylium core. The 6-substituent for the derivatives in Chart 1 is an alkyl group: methyl, *n*-butyl, or *tert*-butyl. Related thiopyrylium compounds **46** and **47** (Chart 4) with methyl and *n*-propyl substituents at the 6-position also displayed inhibitory activity toward P-gp at 25 μM (74 and 87% inhibition, respectively).[26] Structures within this class appear to interact more strongly with MRP1 than with P-gp.

The telluropyrylium compounds **25−27** of class IV (Chart 1) share structural similarities with the class I compounds. These molecules have three aromatic groups at the 2-, 4-, and 6-positions, with at least two of these bearing a 4-aminophenyl and/or a 4-*N*-morpholinophenyl substituent. Whether the aminoaryl substituents are located at the 2,4- or 2,6-positions of the chalcogenopyrylium core, N···N distances will be comparable as well as dihedral angles between the aromatic substituents and the chalcogenopyrylium core. One might expect these compounds to exhibit similar modulatory characteristics as

Table 4. Scoring Summary for Modulation/Inhibition of MRP1 and P-gp by Chalcogenopyrylium Compounds[a]

Compd	MRP1	P-gp
2	++	+
3	+++	++
4	+++	+
5	+++	−
25	+++	−
27	++	+
21	+++	+
22	+++	− − −
23	−	++
6-12	−, − −	−, − −
13	−	++
14	−	+
18	++	−
19	++	− −
20	+	− −
21	+++	+
28	++	+++
29	−	−
30	++	+++
31	+	++
32	− −	−

[a]For MRP1: (+++) denotes >90% inhibition, (++) denotes 70−89% inhibition, (+) denotes 50−69% inhibition, (−) denotes 30−49% inhibition, and (− −) denotes <30% inhibition in the one-dose assays of Tables 1 and 2. For PGP: (+++) denotes K_M < 10 μM, (++) denotes K_M of 10−19 μM, (+) denotes K_M of 20−49 μM, (−) denotes K_M of 50−74 μM, (− −) denotes K_M of 75−199 μM, and (− − −) denotes K_M > 200 μM from the data of Tables 1 and 2.

those observed for the class I compounds and, indeed, compounds **25** and **27** both strongly inhibited MRP1-mediated transport at 30 μM (Tables 1 and 4). The interactions of these two compounds with P-gp appear to be weaker than the interactions with MRP1 (Tables 1 and 4). The thiopyrylium compounds **48−50**, which are closely related in structure to compounds **25−27**, inhibited **VER**-induced P-gp ATPase activity with IC$_{50}$ values of 30, 3.1, and 11 μM, respectively (Chart 4).[26]

The class II compounds **6−20** (Chart 1) are characterized by identical substituents at the 2- and 6-positions of the chalcogenopyrylium core. With the exception of compound **17** with 2,6-diphenyl substituents, the remaining compounds in class II have *tert*-butyl substituents at the 2- and 6-positions.

Chart 4. Structures of Thiopyrylium Compounds with Modulatory/Inhibitory Activity toward P-gp
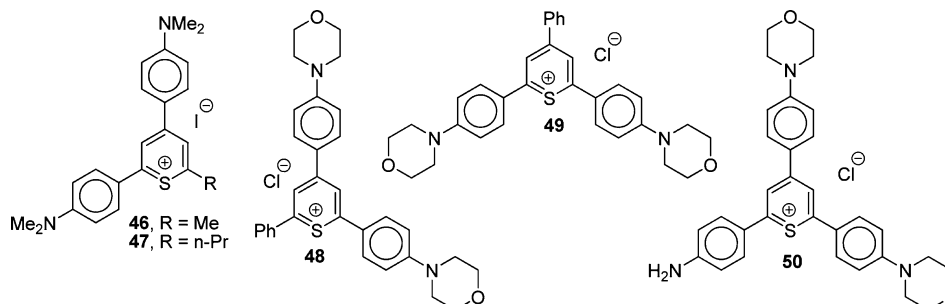
Among the class II compounds, **6–14** and **18–20** were evaluated with both MRP1 and P-gp. Compounds **6–12** were all weak inhibitors of MRP1. Compounds **13** and **14** with *N,N*-diethyl benzamide functionality at the 4-position were weak inhibitors of MRP1 and better modulators of P-gp (Tables 1 and 4). Compounds **18–20** with thioamide functionality at the 4-position were inhibitors of MRP1 and weak modulators of P-gp (Tables 1 and 4).

Compounds **6**, **9**, and **12** exhibited weak but measurable inhibition of MRP1-mediated uptake of [³H]E₂17βG into inside-out membrane vesicles at 30 μM, while these same compounds showed no inhibition of P-gp at 25 μM with respect to **CAM** uptake into MDCKII-MDR1 transfected cells (Table 1). Compound **18**, which exhibited 71% inhibition of [³H]E₂17βG transport by MRP1 at 30 μM, exhibited only 27% inhibition of P-gp at 25 μM in the **CAM** uptake assay (Table 1). These results suggest that the 2,6-di-*tert*-butyl-substituted derivatives among the class II compounds may have differences in both binding to and inhibiting the activity of MRP1 and P-gp.

In the class I and class IV compounds, two aminoaryl substituents gave chalcogenopyrylium compounds that inhibited both P-gp and MRP1, while in the class II compounds, two *tert*-butyl substituents gave compounds with mixed effects. The class III compounds **21–24** (Chart 1) have one *tert*-butyl substituent at the 2-position and one 4-*N,N*-dimethylaminophenyl substituent at the 6-position of the chalcogenopyrylium core. The functionality at the 4-position was diverse with thioamide (**21**) and amide (**23**) hydrogen bond acceptors, carboxylic acid (**22**) hydrogen bond donors, and an unsubstituted phenyl substituent (**24**). Among these compounds, **21** and **22** are strong inhibitors of MRP1-mediated [³H]E₂17βG uptake at 30 μM while compounds **23** and **24** are less inhibitory toward MRP1 at 30 μM but still have measurable inhibition (Tables 1 and 4). Interactions of **21** and **23** with P-gp followed similar trends. Compound **21** exhibited 74% inhibition of P-gp at 25 μM in the **CAM** uptake assay, while compound **23** exhibited only 13% inhibition of P-gp at 25 μM in the same assay (Tables 1 and 4).

Role of the Chalcogen Atom in Modulatory/Inhibitory Behavior of Chalcogenopyrylium Compounds toward MRP1 and P-gp. Several S, Se, Te-triads (**3–5**, **6–8**, **9–11**, **12–14**, and **18–20**) are present in the compounds of Chart 1. As shown in Table 1, all three chalcogen derivatives behaved similarly with respect to inhibition of MRP1-mediated uptake of [³H]E₂17βG into inside-out membrane vesicles. Thus, the identity of the chalcogen atom in the chalcogenopyrylium does not influence the inhibitory behavior of these materials.

With respect to P-gp ATPase activity, the chalcogen atom is similarly inconsequential because K_M values for the three chalcogen analogues were either comparable or their differences followed no predictable order (Table 1). In the **3–5** triad, the thiopyrylium compound **3** has the lower K_M for human P-gp-His₁₀ by a factor of 2.5 relative to selenopyrylium compound **4** and by a factor of 4.5 relative to telluropyrylium compound **5**, i.e., the rank order of the K_M values for this triad is Te > Se > S. The thiopyrylium compound **18** also has the lowest K_M value in the **18–20** triad by a factor of 2 relative to selenopyrylium compound **19** and a factor of 1.6 relative to telluropyrylium compound **20**, giving a rank order of the K_M values of Se > Te > S. In other triads, the selenopyrylium analogue had the lowest K_M value. In the **12–14** triad, the K_M for selenopyrylium compound **13** was roughly half that for telluropyrylium compound **14** and roughly one-third that for thiopyrylium compound **12** and, thus, the rank order of the K_M, values of this triad is S > Te > Se. Within these triads, the variability of V_{max} within each triad is (overall low to high) 2-fold or less, again suggesting minimal impact from the individual chalcogen atoms (Table 1).

Effect of Thiopyrylium Compounds 21 and 28–32 on MRP1 and P-gp Activities. This series of compounds **21** and **28–32** permitted the examination of reactivity with very well-defined structural changes. All six compounds have a thiopyrylium core and allow systematic examination of class II, class III, and class IV substituent changes. As shown in Table 2 and summarized in Table 4, the most efficacious inhibitor of MRP1-mediated [³H]E₂17βG uptake is the class III-related compound **21** while the class II related compounds **29** and **32** (*tert*-Bu substituents at the 2- and 6-positions) give the least inhibition. Class IV-related compounds **28** and **30** also are effective inhibitors of MRP1, while thiopyrylium compound **31** is somewhat less effective.

Interestingly, the effectiveness of compounds **21** and **28–32** as inhibitors of MRP1-mediated [³H]E₂17βG uptake correlates with lipophilicity as indicated by the experimental values of log *P* found in Table 2. Compounds **21**, **28**, **30**, and **31** are the most effective inhibitors of MRP1 with values of log *P* in the 1.4–2.1 range, while compounds **29** and **32** with the lowest values of log *P* (0.7 and 0.2, respectively) are the least effective inhibitors.

The reactivity patterns with P-gp were quite similar. As observed for MRP1 inhibition, the class II-related compounds **29** and **32** had the least effect on P-gp activity and the highest values of K_M (Tables 2 and 4), while class IV-related thiopyrylium compound **30** interacts most strongly with P-gp (lowest K_M and the lowest IC₅₀ value for **VIN** and **CAM** uptake (Table 2)). The activity of compound **30** is followed by class IV-related compounds **28** and **31** with respect to K_M values, IC₅₀ value for **VIN** uptake for **28**, and IC₅₀ values for **CAM** uptake (Tables 2 and 4).

One difference in reactivity pattern was noted. Compound **21**, which most strongly affected MRP1 activity (Tables 1 and 4), was less effective than **28**, **30**, and **31** with respect to inhibiting P-gp based on values of K_M, IC_{50} for **VIN** uptake, and IC_{50} for **CAM** uptake (Tables 2 and 4). Interactions of **21** and **28–32** with P-gp showed no correlations with values of log P.

Thioamide vs Amide Functionality. In the series of compounds **21** and **28–32**, the amide or thioamide substituent at the 4-position impacts inhibitory activity. In a recent study in the laboratories of M. Wiese, thiourea functionality imparted greater inhibitory activity toward MRP1 in a series of drug derivatives relative to P-gp or BCRP.[57] Among the class III-related compounds, the thioamide **21** displays greater inhibition than the corresponding amide **31** with respect to MRP1-mediated [³H]E₂17βG uptake into inside-out membrane vesicles as does the class II thioamide **29** with respect to amide **32** (Tables 2 and 4). The amide and thioamide functionalities resulted in similar inhibition of MRP1 transport activity when class IV-related compounds **28** and **30** at 10 μM are compared (Table 2). With respect to effects on P-gp transport activity, compounds with amide substituents were more efficacious because K_M and IC_{50} values for **CAM** uptake were lower for amide-containing compounds **30** and **31** than for the thioamide-containing compounds **21** and **28** (Table 2).

These observations were also supported by the impact of amide-containing compounds **13**, **14**, and **23** and thioamide-containing compounds **18–20**. The amide-containing compounds **13**, **14**, and **23** interacted weakly with MRP1 but were moderate inhibitors of P-gp (Tables 1 and 4). In contrast, the thioamide-containing compounds **18–20** were strong inhibitors of MRP1 and were weak modulators of P-gp (Tables 1 and 4).

The amide functionality in **13**, **14**, **23**, and **30–32** offers a better hydrogen-bond acceptor and a stronger dipole than the thioamide functionality in **18–21**, **28**, and **29** while conversely, the thioamide groups are more hydrophobic and less polar. For chalcogenopyrylium compounds **1–32**, interactions with MRP1 appear to be favored by the presence of a thioamide group while interactions with P-gp are favored by the presence of an amide group. These differences are not evident in experiments, demonstrating **21** and **28–32** transport across monolayers of MDCKII-MDR1 cells. All six compounds show very slow passive transport ($P_{Passive} \leq 14$ nm s^{-1}) and absorptive transport ($P_{AB} \leq 5.6$ nm s^{-1}) (Table 3). The slowest secretory transport rates (P_{BA}, Table 3) were exhibited by thioamide **28** and amide **31** while thioamide **29** and amide **30** ($P_{BA} \geq 300$ nm s^{-1}) exhibited fast secretory rates, which were only slower than thioamide **21** ($P_{BA} = 620$ nm s^{-1}).

CONCLUSIONS

We have demonstrated that within the series of chalcogenopyrylium compounds **1–32** studied herein, inhibitors of both MRP1 and P-gp activities were identified. Pyrylium, thiopyrylium, selenopyrylium, and telluropyrylium derivatives were examined and the identity of the chalcogen atom shown to have minimal impact on this modulatory activity. The implications here support the idea that effective selenopyrylium and/or telluropyrylium photosensitizers for the PDT of multidrug-resistant cells can be designed based on the SAR of pyrylium and thiopyrylium analogues, which are somewhat easier to synthesize. 4-Aminoaryl substituents on the chalcogenopyrylium ring appear to be important for inhibitory activity in both proteins, while substituent changes at the 2-, 4-, and 6-positions of the chalcogenopyrylium compounds impact the two

transporters differently. This is perhaps not surprising because MRP1 and P-gp share very limited (approximately 15%) homology and are functionally distinct in many ways.[17]

In the 4-position, a thioamide imparts greater inhibitory efficacy than an amide in MRP1, while in P-gp, an amide imparts greater inhibitory efficacy than a thioamide. With respect to P-gp, the differences in inhibitory activity between amide and thioamide groups in the 4-position are opposite to the effects observed in an earlier study of rosamine/rhodamine structures as modulators/inhibitors of P-gp, where a thioamide was more inhibitory than the corresponding amide.[25] These data suggest that the pyrylium structures may bind to a different site on P-gp than do the rosamine/rhodamine structures. Like MRP1,[58] P-gp has been shown to have multiple drug-binding sites[59] and binding could occur through an "induced-fit mechanism" where the chalcogenopyrylium scaffold is more flexible than the rhodamine scaffold.[60,61]

From the structure–activity relationships developed here, comparison of the effectiveness of S-, Se-, and Te-containing analogues of the amide/thioamide-containing structures **13**, **14**, **18–21**, and **28–32** as photosensitizers for the treatment of MRP1- and P-gp-expressing cells by PDT would be of interest. Inactivation of the efflux pump by PDT might allow a dual treatment modality involving both PDT and conventional chemotherapy.

■ EXPERIMENTAL SECTION

General Methods. Chalcogenopyrylium compounds **1–5**,[24,25] **15–17**,[26,30] and **25–27**[32] were prepared by literature methods. Reactions were run under Ar. Tetrahydrofuran was distilled from sodium benzophenone ketyl prior to use. Concentration in vacuo was performed on a Büchi rotary evaporator. NMR spectra were recorded on an Inova 500 instrument (500 MHz for ¹H, 125 MHz for ¹³C) with residual solvent signal as internal standard. Infrared spectra were recorded on a Perkin-Elmer FTIR instrument. UV–vis near-IR spectra were recorded on a Perkin-Elmer Lambda 12 spectrophotometer or on a Shimadzu UV-3600 spectrophotometer in quartz cuvettes with a 1 cm path length. Melting points were determined with a Büchi capillary melting point apparatus and are uncorrected. All compounds tested have a purity of at least 95%, which was determined by an analysis on a C18 reverse-phase HPLC column [Protein RP] using 75% CH₃CN/H₂O with a flow rate of 0.4 mL min^{-1} and monitoring by a UV–visible detector operating at 254 or 442 nm. Nonhygroscopic compounds have a purity of ≥95% as determined by elemental analyses for C, H, and N, which were performed by Atlantic Microlab, Inc., Norcross, GA. Experimental values of C, H, and N are within 0.4% of theoretical values.

2,6-Di-*tert*-butyl-4-phenylthiopyrylium Bromide (6). 2,6-Di-*tert*-butyl-4*H*-thiopyran-4-one (**33-S**, 0.10 g, 0.46 mmol) was dissolved in dry THF (4.5 mL). Phenylmagnesium bromide (5.5 M, 0.96 mL, 5.4 mmol) was added to the solution of **33-S**. The reaction was heated at reflux for 1 h and then cooled to 0 °C. The reaction was quenched by the dropwise addition of 48% HBr (5 mL), and the resulting mixture was stirred 1 h at 0 °C and was then poured into 25 mL of water. The pyrylium compound was extracted with CH₂Cl₂ (3 × 20 mL). The combined organic extracts were washed with water (2 × 15 mL), washed with brine (2 × 15 mL), dried over Na₂SO₄, and concentrated. The residue was recrystallized from CH₃CN/diethyl ether to give 0.064 g (40%) of **6** as a yellow powder, mp 206–209 °C. ¹H NMR [400 MHz, CD₂Cl₂] δ 8.72 (s, 2 H), 8.055 (d × d, 2 H, J = 1.2, 8.0 Hz), 7.72 (m, 3 H), 1.74 (s, 18 H). ¹³C NMR [300 MHz, CD₃CN] δ 185.53, 162.12, 137.82, 133.85, 131.56, 130.78, 118.23, 43.01, 31.18. HRMS (ES) m/z 285.1680 (calcd for C₁₉H₂₅S⁺: 285.1671); λ_{max} (EtOH) 357 nm (ε 2.56 × 10⁴ M^{-1} cm^{-1}). Anal. Calcd for C₁₉H₂₅S·Br: C, 62.46; H, 6.90. Found: C, 62.11; H, 6.96.

2,6-Di-*tert*-butyl-4-phenylselenopyrylium Bromide (7). 2,6-Di-*tert*-butyl-4*H*-selenopyran-4-one (**33-Se**, 0.10 g, 0.37 mmol) and

5.5 M PhMgBr (0.80 mL, 4.4 mmol) were treated as described for the preparation of **6**. The crude product was recrystallized from CH$_3$CN/ diethyl ether to yield 0.085 g (56%) of **7** as an orange powder, mp 198–201 °C. ^{1}H NMR [400 MHz, CD$_2$Cl$_2$] δ 8.53 (s, 2 H), 7.92 (d × d, 2 H, J = 1.2, 8.4 Hz), 7.72 (m, 3 H), 1.743 (s, 18 H). ^{13}C NMR [300 MHz, CD$_3$CN] δ198.15, 162.10, 139.73, 133.36, 131.59, 130.68, 118.26, 44.56, 31.67. HRMS (ES) m/z 333.1122 (calcd for C$_{19}$H$_{25}$[80]Se$^+$: 333.1116); λ_{max} (EtOH) 373 nm (ε 2.2 × 10^4 M^{-1} cm^{-1}). Anal. Calcd for C$_{19}$H$_{25}$Se·Br: C, 55.35; H, 6.11. Found: C, 55.05; H, 6.03.

2,6-Di-*tert*-butyl-4-phenyltelluropyrylium Bromide (8). 2,6-Di-*tert*-butyl-4*H*-telluropyran-4-one (**33-Te**, 0.13 g, 0.40 mmol) and PhMgBr (0.87 mL, 4.8 mmol) were treated as described for the preparation of **6**. The crude product was recrystallized from CH$_3$CN/ diethyl ether to yield 0.083 g (45%) of product as a light-green powder, mp 169–171 °C. ^{1}H NMR [400 MHz, CD$_2$Cl$_2$] δ 8.29 (s, 2 H), 7.73 (d × d, 2 H, J = 1.2, 8.0 Hz), 7.595 (m, 3 H), 1.71 (s, 18 H). ^{13}C NMR [300 MHz, CD$_3$CN] δ 143.01, 135.08, 134.93, 131.41, 130.65, 129.40, 129.33, 45.76, 33.94, 32.22, 32.05, 28.19, 26.29. HRMS (ES) m/z 383.1017 (calcd for C$_{19}$H$_{25}$[130]Te$^+$: 383.1013); λ_{max} (EtOH) 399 nm (ε 1.81 × 10^4 M^{-1} cm^{-1}). Anal. Calcd for C$_{19}$H$_{25}$Te·Br: C, 49.51; H, 5.47. Found: C, 49.55 ; H, 5.45.

2,6-Di-*tert*-butyl-4-(5-carboxythien-2-yl)thiopyrylium Hexafluorophosphate (9). *t*-BuLi (1.3 M in pentane, 2.59 mL, 3.36 mmol) was added dropwise to 5-bromothiophene-2-carboxylic acid (**35**, 0.264 g, 1.60 mmol) and TMEDA (0.066 mL, 0.44 mmol) dissolved in 2.0 mL of dry tetrahydrofuran at −50 °C under an argon atmosphere. The reaction mixture was stirred at ambient temperature for 45 min. This solution was then transferred via syringe to a solution of thiopyranone **33-S** (0.090 g, 0.40 mmol) dissolved in 9.0 mL of dry THF. After 1 h, the reaction mixture was treated with glacial acetic acid (0.25 mL) and poured into 100 mL of aqueous HPF$_6$ (3.0% w/ w), and the resulting mixture was stirred for 1 h. The dye was extracted with CH$_2$Cl$_2$ (3 × 25 mL). The combined organic extracts were dried over Na$_2$SO$_4$ and concentrated. The residue was dissolved in a minimal amount of CH$_3$CN, which was then diluted with ether (3 mL). The product was collected by filtration to give 0.136 g (71%) of **9** as a yellow solid, mp 239–241 °C. ^{1}H NMR [400 MHz, CD$_2$Cl$_2$] δ 8.59 (s, 2 H), 8.16 (d, 1 H, J = 4.0 Hz), 8.04 (d, 1 H, J = 4.0 Hz), 1.68 (s, 18 H). ^{13}C NMR [300 MHz, CD$_3$CN] δ 185.60, 153.17, 145.54, 143.71, 135.76, 135.31, 128.76, 42.84, 30.91. HRMS (ES) m/z 335.1134 (calcd for C$_{18}$H$_{23}$O$_2$S$_2$$^+$:335.1139); λ_{max} (EtOH) 421 nm (ε 2.80 × 10^4 M^{-1} cm^{-1}). Anal. Calcd for C$_{18}$H$_{23}$O$_2$S$_2$·PF$_6$: C, 45.00; H, 4.83. Found: C, 44.91; H, 4.85.

2,6-Di-*tert*-butyl-4-(5-carboxythien-2-yl)selenopyrylium Hexafluorophosphate (10). *t*-BuLi (1.3 M in pentane, 2.6 mL, 3.4 mmol), 5-bromothiophene-2-carboxylic acid (**35**, 0.264 g, 1.60 mmol), TMEDA (0.066 mL, 0.44 mmol), and **33-Se** (0.11 g, 0.40 mmol) were treated as described for the preparation of **9**. The crude product was recrystallized from CH$_3$CN/ether to give 0.144 g (68%) of **10** as a dark-yellow solid, mp 217–223 °C. ^{1}H NMR [400 MHz, CD$_2$Cl$_2$] δ 8.54 (s, 2 H), 8.22 (s, 1 H), 8.02 (s, 1 H), 1.698 (s, 18 H). ^{13}C NMR [300 MHz, CD$_3$CN] δ 162.55, 153.21, 147.52, 138.37, 135.92, 135.59, 135.02, 128.82, 44.46, 31.48. HRMS (ES) m/z 383.0593 (calcd for C$_{18}$H$_{23}$O$_2$S[80]Se$^+$: 383.0584); λ_{max} (EtOH) 449 nm (ε 2.21 × 10^4 M^{-1} cm^{-1}). Anal. Calcd for C$_{18}$H$_{23}$O$_2$SSe·PF$_6$: C, 41.00; H, 4.40. Found: C, 40.93, 4.39.

2,6-Di-*tert*-butyl-4-(5-carboxythien-2-yl)telluropyrylium Hexafluorophosphate (11). *t*-BuLi (1.3 M in pentane, 2.6 mL, 3.4 mmol), 5-bromothiophene-2-carboxylic acid (**35**, 0.264 g, 1.60 mmol), TMEDA (0.066 mL, 0.44 mmol), and **33-Te** (0.13 g, 0.40 mmol) were treated as described for the preparation of **9**. The crude product was recrystallized from CH$_3$CN/ether to give 0.17 g (74%) of a brown solid, mp 215–218 °C. ^{1}H NMR [400 MHz, CD$_2$Cl$_2$] δ 8.61 (s, 2 H), 8.18 (s, H), 7.98 (s, 1 H), 3.46 (s, 1 H), 1.69 (s, 18 H). ^{13}C NMR [300 MHz, DMSO] δ 167.67, 162.67, 147.32, 139.34, 135.03, 133.42, 132.50, 127.34, 33.85, 27.38. HRMS (ES) m/z 433.0459 (calcd for C$_{18}$H$_{23}$O$_2$S[130]Te$^+$: 433.0481); λ_{max} (EtOH) 471 nm (ε 2.64 × 10^4 M^{-1} cm^{-1}). Anal. Calcd for C$_{18}$H$_{23}$O$_2$STe·PF$_6$: C, 37.53; H, 4.02. Found: C, 37.29; H, 4.12.

2,6-Di-*tert*-butyl-4-(2-(*N,N*-diethylaminocarbonyl)phenyl)- thiopyrylium Hexafluorophosphate (12). *s*-BuLi (1.3 M in cyclohexane/hexane, 0.77 mL, 1.0 mmol) was added dropwise to a stirring solution of *N,N*-diethylbenzamide (0.177 g, 1.00 mmol) and TMEDA (0.15 mL, 1.0 mmol) dissolved in 8.0 mL of dry THF at −78 °C. A solution of thiopyranone **33-S** (0.112 g, 0.5 mmol) dissolved in 1.0 mL of dry THF was then added to the benzamide solution via cannula. The reaction mixture was stirred at ambient temperature for 1 h and was then quenched with glacial acetic acid (0.25 mL). The reaction mixture was poured into 100 mL of aqueous HPF$_6$ (3.0% wt/wt) and stirred for 1 h. The crude **12** was extracted with CH$_2$Cl$_2$ (3 × 25 mL). The combined organic extracts were dried over Na$_2$SO$_4$ and concentrated. The residue was recrystallized from CH$_3$CN/ether to give 0.123 g (47%) of a purple−brown solid, mp 180−183 °C. ^{1}H NMR [400 MHz, CD$_2$Cl$_2$] δ 8.63 (s, 2 H), 7.72 (m, 2 H), 7.65 (m, 1 H), 7.50 (m, 1 H), 3.39 (q, 2 H, J = 7.2 Hz), 3.05 (q, 2 H, J = 7.2 Hz), 1.66 (s, 18 H), 1.06 (t, 3 H, J = 7.2 Hz), 0.91 (t, 3 H, J = 7.2 Hz). ^{13}C NMR [300 MHz, CD$_3$CN] δ 186.06, 161.88, 138.12, 135.76, 133.30, 132.55, 131.75, 130.63, 130.44, 128.40, 43.84, 43.04, 39.75, 31.06, 14.12, 13.05. HRMS (ES) m/z 384.2356 (calcd for C$_{24}$H$_{34}$NOS$^+$: 384.2361); λ_{max} (EtOH) 329 nm (ε = 1.50 × 10^4 M^{-1} cm^{-1}). Anal. Calcd for C$_{24}$H$_{34}$NOS·PF$_6$: C, 54.43; H, 6.47; N, 2.64. Found: C, 54.16; H, 6.62; N, 2.67.

2,6-Di-*tert*-butyl-4-(2-(*N,N*-diethylaminocarbonyl)phenyl)- selenopyrylium Hexafluorophosphate (13). *s*-BuLi (1.3 M in cyclohexane/hexane, 0.77 mL, 1.0 mmol), *N,N*-diethylbenzamide (0.177 g, 1.00 mmol), TMEDA (0.15 mL, 1.0 mmol), and seleno- pyranone **33-Se** (0.136 g, 0.50 mmol) were treated as described for the preparation of **12**. The crude product was recrystallized from CH$_3$CN to give 0.058 g (23%) of **13** as a purple−brown solid, mp 155−157 °C. ^{1}H NMR [400 MHz, CD$_2$Cl$_2$] δ 8.535 (s, 2 H), 7.71 (m, 2 H), 7.62 (d, 1 H, J = 7.2 Hz), 7.50 (d × d, 1 H, J = 2.0, 7.8 Hz), 3.37 (q, 2 H, J = 7.2 Hz), 3.01 (q, 2 H, J = 7.2 Hz) 1.68 (s, 18 H), 1.02 (t, 3 H, J = 7.2 Hz), 0.88 (t, 3 H, J = 7.2 Hz). ^{13}C NMR [300 MHz, CD$_3$CN] δ 199.37, 169.42, 161.89, 137.85, 137.41, 133.35, 132.21, 131.33, 130.60, 128.39, 44.69, 43.64, 39.50, 31.57, 14.06, 12.99. HRMS (ES) m/z 432.1808 (calcd for C$_{24}$H$_{34}$NO[80]Se$^+$: 432.1806); λ_{max} (EtOH) 344 nm (ε 1.40 × 10^4 M^{-1} cm^{-1}). Anal. Calcd for C$_{24}$H$_{34}$NOSe·PF$_6$: C, 50.00; H, 5.94; N, 2.43. Found: C, 49.76; H, 5.96; N, 2.54.

2,6-Di-*tert*-butyl-4-(2-(*N,N*-diethylaminocarbonyl)phenyl)- telluropyrylium Hexafluorophosphate (14). *s*-BuLi (1.3 M in cyclohexane/hexane, 0.77 mL, 1.0 mmol), *N,N*-diethylbenzamide (0.177 g, 1.00 mmol), TMEDA (0.15 mL, 1.0 mmol), and telluro- pyranone **33-Te** (0.160 g, 0.50 mmol) were treated as described for the preparation of **12**. The crude product was recrystallized from CH$_3$CN to give 0.077 g (25%) of a dark yellow−green solid, mp 174− 175 °C. ^{1}H NMR [400 MHz, CD$_2$Cl$_2$] δ 8.52 (s, 2 H), 7.68 (m, 2 H), 7.57 (d, 1 H, J = 7.5 Hz), 7.47 (d, 1H, J = 7.5 Hz), 3.33 (q, 2 H, J = 7.2 Hz), 2.94 (q, 2 H, J = 7.2 Hz), 1.66 (s, 18 H), 0.945 (t, 3 H, J = 7.2 Hz), 0.82 (t, 3 H, J = 7.2 Hz). ^{13}C NMR [300 MHz, CD$_3$CN] δ 208.15, 169.61, 161. 49, 139.88, 137.19, 136.90, 131.38, 130.55, 130.42, 128.33, 46.75, 43.39, 39.17, 32.44, 14.03, 13.03. HRMS (ES) m/z 482.1679 (calcd for C$_{24}$H$_{34}$NO[130]Te$^+$: 482.1703); λ_{max} (EtOH) 383 nm (ε 1.48 × 10^4 M^{-1} cm^{-1}). Anal. Calcd for C$_{24}$H$_{34}$NOTe·PF$_6$: C, 46.11; H, 5.48; N, 2.24. Found: C, 45.98; H, 5.60; N, 2.32.

2,6-Di-*tert*-butyl-4-(5-(piperidine-1-carbonothioyl)thiophen- 2-yl)thiopyrylium Hexafluorophosphate (18). Lithium diisopro- pylamide (LDA) was prepared by adding *n*-BuLi (2.0 M in cyclohexane, 0.68 mL, 1.4 mmol) to a solution of diisopropylamine (0.20 mL, 1.4 mmol) in 4.0 mL of dry THF at 0 °C. The solution was stirred for 15 min and then cooled to −78 °C, and piperidin-1-yl- thien-2-yl-methanethione (**38**, 0.284 g, 1.34 mmol), dissolved in 2.0 mL of dry tetrahydrofuran, was added via syringe. The reaction mixture was stirred for 30 min, and an aliquot (1.55 mL, 0.31 mmol) was added via syringe to thiopyranone **33-S** (0.045 g, 0.20 mmol) dissolved in 4.5 mL of dry THF. The reaction mixture was stirred for 30 min at ambient temperature. The mixture was then quenched with glacial acetic acid (0.25 mL), poured into 100 mL of aqueous HPF$_6$ (3.0% w/w), and stirred for 1 h. The crude **18** was extracted with CH$_2$Cl$_2$ (3 × 25 mL). The combined organic extracts were dried over

MgSO$_4$ and concentrated. The resulting residue was purified via column chromatography on SiO$_2$ eluted with 10% diethyl ether/CH$_2$Cl$_2$, followed by 5% methanol/CH$_2$Cl$_2$ to yield 0.075 g (66%) of a dark-red solid, mp 107−110 °C. ^{1}H NMR [400 MHz, CDCl$_3$] δ 8.43 (s, 2 H), 8.16 (d, 1 H, *J* = 4.0 Hz), 7.20 (d, 1 H, *J* = 4.0 Hz), 4.27 (br s, 2 H), 3.81 (br s, 2 H), 1.78 (s, 6 H), 1.62 (s, 18 H). ^{13}C NMR [300 MHz, CD$_3$CN] δ 184.17, 175.85, 172.51, 155.23, 153.20, 135.12, 128.40, 127.60, 126.00, 59.74, 42.42, 30.72, 24.31. HRMS (ES) *m/z* 418.1695 (calcd for C$_{23}$H$_{32}$NS$_3^+$: 418.1697); λ$_{max}$ (EtOH) 416 nm (ε 1.86 × 10^4 M^{-1} cm^{-1}). Anal. Calcd for C$_{22}$H$_{32}$NS$_3$·PF$_6$: C, 49.01; H, 5.72; N, 2.48. Found: C, 49.00; H, 5.75; N, 2.47.

2,6-Di-*tert*-butyl-4-(5-(piperidine-1-carbonothioyl)thiophen-2-yl)selenopyrylium Hexafluorophosphate (19). *n*-BuLi (2.0 M in cyclohexane, 0.68 mL, 1.4 mmol), diisopropylamine (0.20 mL, 1.4 mmol), piperidin-1-yl-thien-2-yl-methanethione (**38**, 0.284 g, 1.34 mmol), and selenopyranone **33-Se** (0.054 g, 0.20 mmol) were treated as described for the preparation of **18** to give 0.090 g (74%) of **19** as a dark-red solid, mp 102−104 °C. ^{1}H NMR [400 MHz, CDCl$_3$] δ 8.40 (s, 2 H), 8.20 (d, 1 H, *J* = 4.0 Hz), 7.21 (d, 1 H, *J* = 4.0 Hz), 4.27 (br s, 2 H), 3.81 (br s, 2 H), 1.79 (s, 6 H), 1.64 (s, 18 H). ^{13}C NMR [300 MHz, CD$_3$CN] δ 196.32, 187.49, 155.00, 153.50, 143.84, 135.21, 128.80, 127.86, 54.75, 52.10, 44.17, 31.48, 27.50, 26.10, 24.54. HRMS (ES) *m/z* 466.1142 (calcd for C$_{23}$H$_{32}$NS$_2$^{80}Se$^+$ 466.1141); λ$_{max}$ (EtOH) 431 nm (ε 1.57 × 10^4 M^{-1} cm^{-1}). Anal. Calcd for C$_{22}$H$_{32}$NS$_2$Se·PF$_6$: C, 45.24; H, 5.28; N, 2.29. Found: C, 45.42; H, 5.56; N, 2.38.

2,6-Di-*tert*-butyl-4-(5-(piperidine-1-carbonothioyl)thiophen-2-yl)telluropyrylium Hexafluorophosphate (20). *n*-BuLi (2.0 M in cyclohexane, 0.68 mL, 1.4 mmol), diisopropylamine (0.20 mL, 1.4 mmol), piperidin-1-yl-thien-2-yl-methanethione (**38**, 0.284 g, 1.34 mmol), and selenopyranone **33-Te** (0.064 g, 0.20 mmol) were treated as described for the preparation of **18** to give 0.098 g (74%) of a dark-red solid, mp 92−94 °C. ^{1}H NMR [400 MHz, CDCl$_3$] δ 8.47 (s, 2 H), 8.13 (d, 1 H, *J* = 4.0 Hz), 7.16 (d, 1 H, *J* = 4.4 Hz), 4.27 (br s, 2 H), 3.82 (br s, 2 H), 1.78 (s, 6 H), 1.62 (s, 18 H). ^{13}C NMR [300 MHz, DMSO] δ 196.73, 187.74, 164.14, 155.32, 142.37, 134.49, 128.82, 127.86, 53.54, 41.78, 33.35, 31.30, 28.01, 26.66, 22.35. HRMS (ES) *m/z* 516.1044 (calcd for C$_{23}$H$_{32}$NS$_2$^{130}Te$^+$ 516.1038); λ$_{max}$ (EtOH) 486 nm (ε 1.716 × 10^4 M^{-1} cm^{-1}). Anal. Calcd for C$_{23}$H$_{32}$NS$_2$Te·PF$_6$: C, 41.91; H, 4.89; N, 2.12. Found: C, 42.00; H, 4.88; N, 2.21.

2-*tert*-Butyl-6-(4-(dimethylamino)phenyl)-4-(5-(piperidine-1-carbonothioyl)thiophen-2-yl)thiopyrylium Chloride (21) and Hexafluorophosphate (41). *n*-Butyllithium (1.6 M in hexanes, 0.947 mL, 1.39 mmol) was added dropwise to a solution of diisoproplyamine (0.21 mL, 1.5 mmol) in THF (5 mL) at −78 °C. The resulting mixture was stirred for 40 min before it was transferred via cannula into a solution of piperidin-1-yl(thiophen-2-yl)methanethione (**38**, 0.151 g, 0.713 mmol) dissolved in THF (5 mL) at −78 °C. The reaction mixture was stirred 30 min before it was transferred via cannula into a solution of 2-*tert*-butyl-6-(4-(dimethylamino)phenyl)-4*H*-thiopyran-4-one (**40**, 0.100 g, 0.348 mmol) in THF (10 mL) at −78 °C. The resulting mixture was stirred for 15 min at −78 °C before warming to 40 °C and stirred for an additional 15 min. Acetic acid (1 mL) was added dropwise, and the mixture was poured into a 10% v/v solution of cold aqueous HPF$_6$ (100 mL). The crude product was extracted with CH$_2$Cl$_2$ (3 × 100 mL). The combined organic extracts were washed with water (3 × 100 mL), dried over MgSO$_4$, filtered, and concentrated. The crude solid was purified via recrystallization from acetonitrile to give 0.33 g (75%) of the hexafluorophosphate salt **41**, mp 138−140 °C. ^{1}H NMR [400 MHz, CD$_2$Cl$_2$] δ 8.33 (s, 1 H), 7.96 (s, 1 H), 7.94 (d, 1 H, *J* = 3.2 Hz), 7.90 (AA′BB′, 2 H, *J* = 8 Hz), 7.22 (d, 1 H, *J* = 3.2 Hz), 6.88 (AA′BB′, 2 H, *J* = 8 Hz), 4.29 (br s, 2 H), 3.84 (br s, 2 H), 3.22 (s, 6 H), 1.81 (br s, 6 H), 1.60 (s, 9 H). ^{13}C NMR [300 MHz, CD$_2$Cl$_2$] δ 187.6, 175.5, 167.4, 155.5, 153.3, 150.45, 142.5, 135.2, 131.2, 128.1, 123.5, 122.4, 121.3, 113.3, 41.1, 40.7, 31.9, 31.2, 24.4, 23.0, 14.2. HRMS (ES) *m/z* 481.1787 (calcd for C$_{27}$H$_{33}$N$_2$S$_3^+$: 481.1806); λ$_{max}$ (EtOH) 630 nm (ε 1.35 × 10^4 M^{-1} cm^{-1}). Anal. Calcd for C$_{27}$H$_{33}$N$_2$S$_3$·PF$_6$: C, 51.74; H, 5.31; N, 4.47. Found: C, 51.43; H, 5.13; N, 4.21.

Compound **41** (0.126 g, 0.20 mmol) was dissolved in 3 mL of methanol and 0.50 g of Amberlite-400 (Cl) ion-exchange resin

(washed three times with 5 mL of methanol prior to use) was added, and the resulting mixture was stirred for 1 h at ambient temperature. The resin was removed by filtration, and the filter cake was washed with 3 mL of methanol. The exchange was repeated twice more. The final filtrates were concentrated, and the residue was purified via recrystallization from CH$_3$CN to give 0.089 g (71%) of **21** a dark-purple solid, mp 138−140 °C. ^{1}H NMR [400 MHz, CD$_2$Cl$_2$] δ 8.33 (s, 1 H), 7.96 (s, 1 H), 7.94 (d, 1 H, *J* = 3.2 Hz), 7.90 (AA′BB′, 2 H, *J* = 8 Hz), 7.22 (d, 1 H, *J* = 3.2 Hz), 6.88 (AA′BB′, 2 H, *J* = 8 Hz), 4.29 (br s, 2 H), 3.84 (br s, 2 H), 3.22 (s, 6 H), 1.81 (br s, 6 H), 1.60 (s, 9 H). ^{13}C NMR [300 MHz, CD$_2$Cl$_2$] δ 187.6, 175.5, 167.4, 155.5, 153.3, 150.5, 142.5, 135.2, 131.2, 128.1, 123.5, 122.4, 121.3, 113.3, 41.1, 40.7, 31.9, 31.2, 24.4, 23.0, 14.2. HRMS (ES) *m/z* 481.1787 (calcd for C$_{27}$H$_{33}$N$_2$S$_3^+$: 481.1806); λ$_{max}$ (EtOH) 629 nm (ε 1.33 × 10^4 M^{-1} cm^{-1}). Anal. Calcd for C$_{27}$H$_{33}$N$_2$S$_3$Cl: C, 62.70; H, 6.43; N, 5.42. Found: C, 62.43; H, 6.13; N, 5.21.

2-*tert*-Butyl-6-(4-(dimethylamino)phenyl)-4-(5-carboxy-thien-2-yl)-thiopyrylium Hexafluorophosphate (22). *t*-BuLi (1.48 M in pentane, 2.84 mL, 4.22 mmol), 5-bromothiophene-2-carboxylic acid (**35**, 0.331 g, 2.00 mmol), TMEDA (0.080 mL, 0.55 mmol), and thiopyranone **40** (0.13 g, 0.40 mmol) were treated as described for the preparation of **9**. The crude product was recrystallized from CH$_3$CN/ether to give 0.141 g (52%) of **22** as a dark-blue solid, mp 154−156 °C. ^{1}H NMR [400 MHz, (CD$_3$)$_2$SO] δ 8.72 (s, 1 H), 8.56 (d, 1 H, *J* = 4.4 Hz), 8.28 (s, 1 H), 8.18 (d, 2 H, *J* = 9.2 Hz), 7.95 (d, H, *J* = 4.0 Hz), 6.94 (d, 2 H, *J* = 9.2 Hz), 3.18 (s, 6 H), 1.57 (s, 9 H). ^{13}C NMR [300 MHz, CD$_3$CN] δ 177.6, 172.7, 169.1, 162.15, 156.3, 150.2, 146.9, 140.8, 140.8, 135.8, 133.4, 131.3, 124.6, 123.5, 121.5, 113.9, 40.6, 30.9. HRMS (ES) *m/z* 398.1247 (calcd for C$_{22}$H$_{24}$NO$_2$S$_2^+$: 398.1248); λ$_{max}$ (EtOH) 616 nm (ε = 2.83 × 10^4 M^{-1} cm^{-1}). Anal. Calcd for C$_{22}$H$_{24}$NO$_2$S$_2$: C, 48.62; H, 4.45; N, 2.58. Found: C, 48.23; H, 4.41; N, 2.48.

2-*tert*-Butyl-4-(2-(*N,N*-diethylaminocarbonyl)phenyl)-6-(4-(dimethylamino)phenyl)thiopyrylium Bromide (23). *s*-BuLi (1.3 M in cyclohexane/hexane, 0.77 mL, 1.0 mmol), *N,N*-diethylbenzamide (0.177 g, 1.00 mmol), TMEDA (0.15 mL, 1.0 mmol), and thiopyranone **40** (0.144 g, 0.500 mmol) were treated as described for the preparation of **12**. The crude product was recrystallized from CH$_3$CN/ether to give 0.119 g (45%) of **23** as a purple solid, mp 74−75 °C. ^{1}H NMR [400 MHz, CD$_2$Cl$_2$] δ 8.48 (s, 1 H), 8.03 (s, 1 H), 8.00 (d, 1 H, *J* = 6.4 Hz), 7.70 (m, 3 H), 7.47 (m, 2 H), 6.92 (d, 2 H, *J* = 8.8 Hz), 3.41 (q, 2 H, *J* = 7.2 Hz), 3.24 (s, 6 H), 3.00 (q, 2 H, *J* = 7.2 Hz), 1.60 (s, 9 H), 0.98 (t, 3 H, *J* = 7.2 Hz), 0.90 (t, 3 H, *J* = 7.2 Hz). ^{13}C NMR [300 MHz, CD$_3$CN] δ 177.56, 158.69, 136.38, 132.02, 131.24, 130.86, 130.46, 128.70, 128.24, 127.55, 113.95, 43.75, 40.60, 39.60, 30.97, 13.99, 12.84. HRMS (ES) *m/z* 447.2470 (calcd for C$_{28}$H$_{35}$N$_2$OS$^+$: 447.2470); λ$_{max}$ (EtOH) 601 (ε 2.59 × 10^4 M^{-1} cm^{-1}). Anal. Calcd for C$_{28}$H$_{35}$N$_2$OS·Br: C, 64.48; H, 6.12; N, 3.27. Found: C, 64.43; H, 6.09; N, 3.11.

2-*tert*-Butyl-6-(4-(dimethylamino)phenyl)-4-phenylthiopyrylium Bromide (24). 2-*tert*-Butyl-6-(4-(dimethylamino)phenyl)-4*H*-thiopyran-4-one (**40**, 0.14 g, 0.50 mmol) and 5.5 M PhMgBr (1.1 mL, 6.0 mmol) were treated as described for the preparation of **6**. The crude product was recrystallized from CH$_3$CN/ether to give 0.187 g (87%) of **24** as a dark-purple powder, mp >250 °C. ^{1}H NMR [400 MHz, CD$_2$Cl$_2$] δ 8.52 (s, H), 8.08 (s, 2 H), 7.94 (s, 2 H), 7.68 (s, 3 H), 6.92 (d, 2 H, *J* = 4.8 Hz), 3.23 (s, 6 H), 1.64 (s, 9H). ^{13}C NMR [300 MHz, CD$_3$CN] δ 178.23, 169.57, 159.57, 156.04, 138.51, 133.14, 131.37, 130.53, 129.94, 127.47, 126.16, 121.63, 113.76, 41.78, 40.59, 31.05. HRMS (ES) *m/z* 348.1775 (calcd for C$_{23}$H$_{26}$NS$^+$: 348.1786); λ$_{max}$ (EtOH) 595 nm (ε 2.6 × 10^4 M^{-1} cm^{-1}). Anal. Calcd for C$_{23}$H$_{26}$NS·PF$_6$: C, 55.98; H, 5.31; N, 2.84. Found: C, 56.03; H, 5.41; N, 2.83.

2,6-Bis(4-(dimethylamino)phenyl)-4-(5-(piperidine-1-carbonothioyl)thien-2-yl)thiopyrylium Chloride (28) and Hexafluorophosphate (43). *n*-Butyllithium (1.6 M in hexanes, 0.693 mL, 1.02 mmol) was added dropwise to a solution of diisopropylamine (0.17 mL, 1.2 mmol) in THF (5 mL) at −78 °C. The resulting mixture of LDA was stirred for 40 min before it was transferred via cannula into a solution of **38** (0.151 g, 0.713 mmol) dissolved in THF

(5 mL) at −78 °C. The reaction mixture was stirred 30 min before it was transferred via cannula into a solution of 2,6-bis(4-(dimethylamino)-phenyl)-4H-thiopyran-4-one (**42**,[40] 0.100 g, 0.285 mmol) in THF (10 mL) at −78 °C. The resulting mixture was stirred for 15 min at −78 °C and was then warmed to 40 °C and stirred for an additional 15 min. Acetic acid (1 mL) was added dropwise, and the mixture was poured into a 10% v/v solution of cold aqueous HPF_6 (100 mL). The crude product was extracted with CH_2Cl_2 (3 × 100 mL). The combined organic extracts were washed with water (3 × 100 mL), dried over $MgSO_4$, filtered, and concentrated to give the hexafluorophosphate salt **43**, which was recrystallized from CH_3CN to give 0.16 g (80%) of **43**, mp 195−197 °C. ^{1}H NMR [500 MHz, CD_2Cl_2] δ 8.50 (d, 1 H, J = 4.0 Hz), 8.28 (s, 2 H), 7.98 (d, AA′BB′, 4 H, J = 9.0 Hz), 7.22 (d, 1 H, J = 4.0 Hz), 6.89 (d, AA′BB′, 4 H, J = 9.0 Hz), 4.29 (br s, 2 H), 3.86 (br s, 2 H), 3.17 (s, 12 H), 1.80 (m, 6 H). ^{13}C NMR [75.6 MHz, CD_2Cl_2] δ 187.5, 162.5, 154.7, 152.3, 149.3, 142.8, 131.4, 129.4, 127.8, 120.6, 119.2, 113.0, 52.4, 40.4, 27.4, 25.9, 24.4. HRMS (ES) m/z 544.1912 (calcd for $C_{31}H_{34}N_3S_3^+$: 544.1909); λ_{max} (CH_2Cl_2) 716 nm (ε 3.9 × 10^{4} $M^{-1}cm^{-1}$). Anal. Calcd for $C_{31}H_{34}N_3S_3 \cdot PF_6$: C, 53.98; H, 4.97; N, 6.09. Found: C, 54.01; H, 4.95; N, 6.12.

The hexafluorophosphate salt of **43** was exchanged for chloride as described for the preparation of **21**. The final filtrates were concentrated, and the residue was purified via recrystallization from CH_3CN to give 0.062 g (31%) of **28** as a dark-purple solid, mp 190−193 °C. ^{1}H NMR [500 MHz, CD_2Cl_2] δ 8.50 (d, 1 H, J = 4.0 Hz), 8.28 (s, 2 H), 7.98 (d, AA′BB′, 4 H, J = 9.0 Hz), 7.22 (d, 1 H, J = 4.0 Hz), 6.89 (d, AA′BB′, 4 H, J = 9.0 Hz), 4.29 (br s, 2 H), 3.86 (br s, 2 H), 3.17 (s, 12 H), 1.80 (m, 6 H). ^{13}C NMR [75.6 MHz, CD_2Cl_2] δ 187.5, 162.5, 154.7, 152.3, 149.3, 142.8, 131.4, 129.4, 127.8, 120.6, 119.2, 113.0, 52.4, 40.4, 27.4, 25.9, 24.4. HRMS (ES) m/z 544.1912 (calcd for $C_{31}H_{34}N_3S_3^+$: 544.1909); λ_{max} (CH_2Cl_2) 717 nm (ε 3.8 × 10^{4} $M^{-1}cm^{-1}$).

Preparation of 2,6-Di-*tert*-butyl-4-(5-(piperidine-1-carbonothioyl)thiophen-2-yl)thiopyrylium Chloride (29). The hexafluorophosphate salt of **18** was exchanged for chloride as described for the preparation of **21**. The crude solid was purified via recrystallization from CH_3CN to give 0.059 g (29%) of **29** as a dark-red solid, mp 107−110 °C. ^{1}H NMR [500 MHz, CD_2Cl_2] δ 9.02 (s, 2 H), 8.78 (d, 1 H, J = 4.0 Hz), 7.29 (d, 1 H, J = 4.0 Hz), 4.29 (br s, 2 H), 3.84 (br s, 2 H), 1.80 (m, 6 H), 1.68 (s, 18 H). ^{13}C NMR [75.6 MHz, CD_2Cl_2] δ 186.8, 184.0, 156.0, 153.4, 141.1, 135.1, 128.3, 126.7, 52.0, 42.4, 31.3, 30.0, 27.4, 25.8, 24.3. HRMS (ES) m/z 418.1691 (calcd for $C_{23}H_{32}N_1S_3^+$: 418.1691); λ_{max} (EtOH) 416 nm (ε 1.86 × 10^{4} $M^{-1}cm^{-1}$).

2,6-Bis(4-(dimethylamino)phenyl)-4-(5-(piperidine-1-carbonyl)thien-2-yl)thiopyrylium Hexafluorophosphate (30). Thioamide **43** (0.250 g, 0.362 mmol) and trifluoroacetic anhydride (0.50 mL, 3.6 mmol) were treated as described for the preparation of **31**. The crude solid was purified via recrystallization from CH_3CN to give 0.127 g (52%) of **30** as a dark-blue solid, mp 142−145 °C. ^{1}H NMR [500 MHz, CD_2Cl_2] δ 8.14 (s, 2 H), 8.08 (br s, 1 H), 7.875 (d, AA′BB′, 4 H, J = 9.0 Hz), 7.41 (d, 1 H, J = 4.0 Hz), 6.85 (d, AA′BB′, 4 H, J = 9.0 Hz), 3.684 (t, 4 H, J = 6.0 Hz), 3.16 (s, 12 H), 1.73 (m, 6 H). ^{13}C NMR [75.6 MHz, CD_2Cl_2] δ 162.0, 161.4, 154.5, 149.0, 145.3, 142.7, 132.0, 130.7, 129.3, 120.4, 119.1, 112.8, 45.1 (br), 40.2, 26.4, 24.8. HRMS (ES) m/z 528.2130 (calcd for $C_{31}H_{34}O_1N_3S_2^+$: 528.2138); λ_{max} (CH_2Cl_2) 717 nm (ε 4.68 × 10^{4} $M^{-1}cm^{-1}$).

2-*tert*-Butyl-6-(4-(dimethylamino)phenyl)-4-(5-(piperidine-1-carbonyl)thien-2-yl)thiopyrylium Hexafluorophosphate (31). Trifluoroacetic anhydride (0.55 mL, 4.0 mmol) was added dropwise to a stirred solution of hexafluorophosphate salt **41** (0.250 g, 0.339 mmol) dissolved in CH_2Cl_2 (25 mL). The resulting mixture was heated at reflux for 14 h, and then 10% sodium carbonate solution (5 mL) was added dropwise and the reaction was poured into distilled water (200 mL). The crude product was extracted with CH_2Cl_2 (3 × 100 mL). The combined organic extracts were washed with water (3 × 100 mL), dried over Na_2SO_4, and concentrated. The crude solid was purified via recrystallization from CH_3CN to give 0.177 g (73%) of **31** as a blue solid, mp 194−197 °C. ^{1}H NMR [500 MHz, CD_2Cl_2] δ 8.47 (s, 1 H), 8.16 (br s, 1 H), 8.01 (s, 1 H), 7.98 (d, AA′BB′, 2 H,

J = 9.0 Hz), 7.44 (d, 1 H, J = 4.0 Hz), 6.90 (d, AA′BB′, 2 H, J = 9.0 Hz), 3.68 (t, 4 H, J = 6.0 Hz), 3.22 (s, 12 H), 1.73 (m, 6 H), 1.60 (s, 9 H). ^{13}C NMR [75.6 MHz, CD_2Cl_2] δ 176.0, 167.8, 161.4, 155.6, 150.2, 146.7, 142.4, 132.8, 130.8, 130.5, 123.3, 121.9, 121.0, 113.4, 49.9 (br), 41.1, 40.6, 31.1, 26.4, 24.7. HRMS (ESI) m/z 465.2029 (calculated for $C_{27}H_{33}O_1N_2S_2^+$: 465.2029); λ_{max} (CH_2Cl_2) 644 nm (ε 3.67 × 10^{4} $M^{-1}cm^{-1}$).

2,6-Di-*tert*-butyl-4-(5-(piperidine-1-carbonothioyl)thien-2-yl)thiopyrylium Hexafluorophosphate (32). Trifluoroacetic anhydride (0.62 mL, 4.4 mmol) and thioamide **18** (0.25 g, 0.44 mmol) were treated as described for the preparation of **31**. The crude product was recrystallized from acetonitrile to give 0.079 g (34%) of **32** as a copper−brown solid, mp 110−113 °C. ^{1}H NMR [500 MHz, CD_2Cl_2] δ 8.54 (s, 2 H), 8.25 (d, 1 H, J = 4.0 Hz), 7.48 (d, 1 H, J = 4.0 Hz), 3.66 (br s, 4 H), 1.73 (m, 6 H), 1.66 (s, 18 H). ^{13}C NMR [75.6 MHz, CD_2Cl_2] δ 184.5, 161.0, 153.4, 149.2, 141.3, 134.9, 131.1, 127.2, 49.3 (br), 42.4, 31.2, 26.4, 24.6. HRMS m/z 402.1913 (calcd for $C_{23}H_{32}O_1N_1S_2^+$: 402.1920); λ_{max} (CH_2Cl_2) = 442 nm (ε 3.21 × 10^{4} $M^{-1}cm^{-1}$).

Determination of Partition Coefficients. The n-octanol/water partition coefficients were all measured at pH 7.4 in PBS using UV−visible spectrophotometry. The measurements were done using a "shake flask" direct measurement.[41] Mixing for 3−5 min was followed by 1 h of settling time. Equilibration and measurements were made at 23 °C using a Perkin-Elmer Lambda 12 spectrophotometer. High-performance liquid chromatography grade n-octanol was obtained from Sigma-Aldrich.

Cell Culture for MRP1 Studies. A stably transfected MRP1 over-expressing HEK cell line was generated using a pcDNA3.1(−) expression vector containing the entire human MRP1 cDNA transcript.[39] Following transfection using Lipofectamine 2000 (Gibco-Invitrogen; Burlington, ON). HEK cells were selected in G418 (ONBIO; Richmond Hill, ON) (1 mg mL^{-1}), and clones of surviving cells were isolated using colony rings. Clonal cell lines were then expanded and screened for MRP1 by immunoblotting with mouse mAb QCRL-1.[62] Homogeneity of MRP1 expressing cell populations was confirmed by flow cytometry using mouse mAb QCRL-3[63] on an Epics Altra HSS flow cytometer (Beckman Coulter). A homogeneous stable cell line thus obtained was designated HEK-MRP1. All cultured cells were incubated in Dulbecco's Modified Essential Medium with 7.5% fetal bovine serum (FBS) at 37 °C in 5% CO_2/95% air. For membrane vesicle preparations, HEK-MRP1 cells were seeded onto 150 mm plates at 18 × 10^{6} cells per 20 mL and harvested at confluence.

Preparation of MRP1-Enriched Membrane Vesicles. Membrane vesicles were prepared essentially as described by Loe et al.[64] Cell pellets were thawed slowly on ice, resuspended in homogenization buffer [250 mM sucrose/50 mM Tris pH 7.4/0.25 mM $CaCl_2$ with protease inhibitors (Roche, Mississauga, ON)], and disrupted by argon cavitation (350 psi, 4 °C, 5 min). After centrifugation at 1400, the supernatant was transferred to high speed centrifuge tubes and the remaining pellet was resuspended in homogenization buffer with 0.5 mM EDTA. Following a second centrifugation at 1400g, the supernatants from the first and second centrifugations were combined and overlaid onto a cushion comprised of 35% (w:v) sucrose/1 mM EDTA/50 mM Tris, pH 7.4. After centrifugation at 100000g, the interface layer containing membranes was removed, placed in 25 mM sucrose/50 mM Tris, pH 7.4 buffer, and the membranes collected by centrifugation again at 100000g. The membranes were then washed with Tris-sucrose buffer (TSB) (250 mM sucrose, 50 mM Tris, pH 7.4) and centrifuged at 55000g. The pellet was resuspended in TSB and vesicles prepared by passaging through a 1 mL syringe with a 27-gauge needle. Vesicles were stored at −80 °C until needed. Vesicular protein concentrations were determined using the Bradford method with BSA as a standard.

Immunoblotting for MRP1. The presence of MRP1 in the membrane vesicles was confirmed by immunoblot analysis as follows: proteins were resolved by electrophoresis on a 7% polyacrylamide gel and then electrotransferred to polyvinylidene fluoride membranes (Pall Corporation; Ville St. Laurent, QC). After transfer, the membranes were washed in TBS plus 0.1% Tween-20 (TBST) and then blocked in

4% (w:v) skim milk powder in TBST for 1 h. Following blocking, the membranes were incubated overnight at 4 °C with mAb QCRL-1 (diluted 1:10000) in blocking solution.[65] After washing, blots were incubated with horseradish peroxidase-conjugated secondary antibody (Pierce Biotechnology; Rockford, IL) in blocking solution for 1−2 h at room temperature and then washed in TBST before incubating with chemiluminescence blotting substrate (PerkinElmer; Woodbridge, ON) and exposing to film.

MRP1-Mediated Uptake of [^{3}H]E$_2$17βG by Membrane Vesicles. ATP-dependent uptake of [6,7-^{3}H]E$_2$17βG (45 Ci mmol^{-1}) (PerkinElmer,Woodbridge, ON) by MRP1-enriched membrane vesicles was measured using a 96-well rapid filtration method previously described.[65] Reactions were carried out in duplicate in 96-well round-bottomed plates in a final reaction volume of 30 μL TSB. Vesicle protein (2 μg) was incubated with reaction mix containing [^{3}H]E$_2$17βG (400 nM, 20 nCi) for 3 min at 37 °C. Stock solutions of chalcogenopyrylium compounds were diluted as needed in TSB in the dark and then added to both the reaction mix (containing either AMP or ATP (4 mM), MgCl$_2$ (10 mM), and E$_2$17βG/[^{3}H]E$_2$17βG) and the membrane vesicle preparations. The final concentration of DMSO never exceeded 1%. Uptake of [^{3}H]E$_2$17βG was stopped by rapid dilution in ice-cold TSB followed by rapid filtration of the wells' contents onto a Unifilter-96 GF/B filter plate using a 96-well Filtermate Harvester apparatus (Packard BioScience, Meriden, CT). Radioactivity was measured by liquid scintillation counting on a TopCount NXT microplate scintillation and luminescence counter (Perkin-Elmer), and uptake was expressed as pmol [^{3}H]E$_2$17βG mg protein^{-1} min^{-1}. To determine ATP-dependent uptake, uptake in the presence of AMP was subtracted from uptake in the presence of ATP.

Expression and Purification of P-gp, and Measurement of P-gp ATPase Activity. The cDNA for human P-gp[45] was modified to contain a tag of 10 His residues at the COOH-terminus (P-gp-His$_{10}$) to facilitate purification by metal-chelate chromatography.[46] Baby hamster kidney (BHK) cells were cotransfected with P-gp-His$_{10}$ and pWL-neo (Stratagene, Cedar Creek, TX), and the transfected cells selected with G418 as described previously.[66] G418-resistant colonies were selected and clones overexpressing P-gp were identified by subjecting whole cell extracts to immunoblot analysis with a rabbit polyclonal antibody to P-gp.[67] BHK cells overexpressing P-gp-His$_{10}$ were then expanded and used to obtain purified protein.

His-tagged P-gp was isolated by Ni-chelate chromatography as described previously.[46] A sample of the isolated His-tagged P-gp was mixed with an equal volume of 10 mg mL^{-1} sheep brain phosphatidylethanolamine (Type II−S, Sigma) that had been washed and suspended in TBS (Tris-buffered saline: 10 mM Tris/HCl, pH 7.4 and 150 mM NaCl). The sample was sonicated and ATPase activity measured in the absence of drug substrate or in the presence of various concentrations of chalcogenopyrylium compounds. The samples were incubated for 30 min at 37 °C, and the amount of inorganic phosphate released was determined.[47]

To test for inhibition of drug-stimulated P-gp ATPase activity, samples of P-gp-His$_{10}$ in lipid were preincubated with various concentrations of the chalcogenopyrylium compounds for 15 min at 20 °C. The ATPase reactions were then started by addition of ATPase reaction mix containing **VER** (final concentration of 0.4 mM) and ATPase activity determined as described above. **VER** was used to test for inhibition because it is one of the most commonly used and potent stimulators of P-gp ATPase activity.[45]

Enhancement of CAM Uptake into MDCKII-MDR1 Cells by Chalcogenopyrylium Compounds. MDCK cells transfected with wild-type MDR1 (ABCB1) were obtained at passage number 12 from Dr. Piet Borst at The Netherlands Cancer Institute. Cell growth was maintained in Dulbecco's Modified Eagle's Medium (Gibco) supplemented with 10% fetal bovine serum (FBS), 100 units mL^{-1} penicillin, and 100 μg mL^{-1} streptomycin in 75-cm^2 flasks. Cultures were passaged by trypsinization 1:10 twice a week and used at passage numbers 16−42. Cells were seeded at 40000 cells per well in 96-well flat bottom plates (Falcon) using a medium volume of 200 μL, which was replaced on day 3 prior to their use on day 4.

Cells were washed once with Dulbecco's phosphate-buffered saline containing 10 mM HEPES buffer at pH 7.4 (DPBSH) (Gibco) and incubated with solutions of the chalcogenopyrylium analogue or control compound in DPBSH at 37 °C in room atmosphere. IC$_{50}$ values were calculated from 1:1 serial dilution series. After 30 min, the test compound was replaced to include 0.5 μg mL^{-1} CAM and incubated an additional 20 min. Calcein fluorescence was read on a Cytofluor series 4000 Multi Well Plate Reader (PerSeptive Biosystems) with λ_{EX} and λ_{EM} set at 485 and 530 nm, respectively. Negative (0.25% DMSO in DPBSH) and positive [5 μM, **44** (LSN 335984)] controls were included in each plate. IC$_{50}$ values were calculated from the serial dilution curves using GraphPad PRISM version 4.03 software. Briefly, compound concentration was plotted as log μM concentration versus relative fluorescence units (rfu) and a sigmoidal dose−response (variable slope) analysis with no weighting or restrictions was applied. The CAM fluorescence observed with 5 μM **44** was taken as complete inhibition.

P-gp-Mediated Transport across MDCKII-MDR1 Monolayers. MDCKII-MDR1 cells that were seeded at 50000 cells cm^{-2} onto 12-well (1.13 cm^2 surface area) Transwell polycarbonate filters (Costar) were fed on days 3 and 5 and used on day 6. The upper and lower chamber volumes were 0.5 and 1.0 mL, respectively. Cells were rinsed 10 min in DPBSH at 37 °C with mixing on a nutator (Clay Adams). Cells were preincubated with 4.3 mg mL^{-1} BSA in DPBSH alone or containing 5 μM **44** (LSN 335984). After 30 min, 5 μM test compound (**21, 28−32**) in BSA/DPBSH with or without the inhibitor **44** was added to the donor chamber (0.5 mL upper or apical, 1.0 mL lower or basolateral). Initial samples from the donor chamber were taken at t = 0. For apical-to-basolateral (AB) flux, D_0 was taken from the mixing tube before addition to the cell monolayer. For basolateral-to-apical (BA) flux, the sample was taken from the 12-well plate 10 min after transfer but before cell wells were added. Samples were taken from both the donor and receiver chambers following a 1 h incubation at 37 °C with constant mixing by nutation. Cell monolayers were rinsed briefly twice with cold DPBS and extracted with 500 μL of methanol for 3 min. Fifty μL samples (n = 3) were placed in a 96-deep well assay plate, and protein was precipitated by adding 450 μL of acetonitrile and shaken to mix. Plates were centrifuged 5 min at 5000 rpm. Compound concentrations were determined with an LC-MS/MS assay. Chromatography was performed using a Betasil C18 2 mm × 20 mm 5 μm Javelin column (Thermo Scientific, Waltham, MA) and 1 of 2 mobile phase systems. System 1 consisted of 5 mM ammonium bicarbonate in water (mobile phase A) and 5 mM ammonium bicarbonate in methanol (mobile phase B), with elution accomplished by a methanol gradient at 1.5 mL min^{-1}. System 2 consisted of 0.4% trifluoracetic acid (TFA), 1 mM ammonium bicarbonate in water (mobile phase A), and 0.4% TFA/1 mM ammonium bicarbonate in acetonitrile (mobile phase B), with elution accomplished by an acetonitrile gradient at 1.5 mL min^{-1}. Mass spectrometric detection was performed with an API4000 mass spectrometer (Applied Biosystems, Foster City, CA) equipped with a turbo ion spray source, using selected reaction monitoring in positive ion mode with precursor and product ion transitions specific to each analyte.

Inhibition of VIN Efflux from MDCKII-MDR1 Cells by Chalcogenopyrylium Compounds 21, 28, and 30. MDCKII-MDR1 cells were seeded onto Costar Transwell polycarbonate membranes and maintained as described above. On day 6, cells were rinsed once for 10 min in DPBSH with nutation at 37 °C and then were exposed to 0.0001, 0.01, 0.05, 0.1, 0.5, 1, or 10 μM **21, 28,** or **30** in BSA/DPBSH. After 30 min at 37 °C, 1.0 mL [^{3}H]-**VIN** (0.25 μCi mL^{-1} from 0.1 mCi mL^{-1} ethanol stock) in appropriate 0.0001, 0.01, 0.05, 0.1, 0.5, 1, or 10 μM **21, 28,** or **30** solution was introduced to the basolateral chamber and 0.5 mL of fresh 0.0001, 0.01, 0.05, 0.1, 0.5, 1, or 10 μM chalcogenopyrylium solution was added to the apical chamber. Initial donor samples were taken from the basolateral chamber at t = 0. The apical solution was replaced every 10 min with fresh buffer, and appearance of [^{3}H]-**VIN** in the apical chamber was measured by scintillation counting. An IC$_{50}$ was calculated using XLfit software.

AUTHOR INFORMATION

Corresponding Author
*Phone: (716) 645-4228. Fax: (716) 645-6963. E-mail: mdetty@buffalo.edu.

Notes
The authors declare no competing financial interest.

ACKNOWLEDGMENTS

ABBREVIATIONS USED

ABC, ATP-binding cassette; BCRP, breast cancer resistance protein; BHK, baby hamster kidney; BSA, bovine serum albumin; CAM, calcein AM; DMSO, dimethylsulfoxide; DPBSH, Dulbecco's HEPES-containing phosphate-buffered saline; $E_2 17\beta G$, estradiol glucuronide; FBS, fetal bovine serum; HEK, human embryonic kidney; LDA, lithium diisopropylamide; MDCK, Madin–Darby canine kidney; MDR, multidrug resistance; MRP, multidrug resistance protein; NBD, nucleotide binding domain; P-gp, P-glycoprotein; TBS, Tris-buffered saline; THF, tetrahydrofuran; TMD, transmembrane domain; TMEDA, tetramethylethylenediamine; TSB, Tris sucrose buffer; TBST, TBS plus 0.1% Tween-20; VER, verapamil; VIN, vinblastine

REFERENCES

(1) Gottesman, M. M.; Fojo, T.; Bates, S. E. Multidrug resistance in cancer: role of ATP-dependent transporters. *Nature Rev. Cancer* **2002**, *2*, 48−58.

(2) Szakacs, G.; Paterson, J. K.; Ludwig, J. A.; Booth-Genthe, C.; Gottesman, M. M. Targeting multidrug resistance in cancer. *Nature Rev. Drug Discovery* **2006**, *5*, 219−234.

(3) Dean, M.; Rzhetsky, A.; Allikmets, R. The human ATP-binding cassette (ATP) transporter superfamily. *Genome Res.* **2001**, *11*, 1156−1165.

(4) Huang, Y.; Sadée, W. Membrane transporters and channels in chemoresistance and -sensitivity of tumor cells. *Cancer Lett.* **2006**, *239*, 168−182.

(5) Sharom, F. J. ABC multidrug transporters: structure, function and role in chemoresistance. *Pharmacogenomics* **2008**, *9*, 105−127.

(6) Bhatia, A.; Schäfer, H.-J.; Hrycyna, C. A. Oligomerization of the human ABC transporter ABCG2: evaluation of the native protein and chimeric dimers. *Biochemistry* **2005**, *44*, 10893−10904.

(7) Gottesman, M. M.; Ling, V. The molecular basis of multidrug resistance in cancer: the early years of P-glycoprotein research. *FEBS Lett.* **2006**, *580*, 998−1009.

(8) Ambudkar, S. V.; Dey, S.; Hrycyna, C. A.; Ramachandra, M.; Pastan, I.; Gottesman, M. M. Biochemical, cellular, and pharmacological aspects of the multidrug transporter. *Annu. Rev. Pharmacol. Toxicol.* **1999**, *39*, 361−368.

(9) Aller, S. G.; Yu, J.; Ward, A.; Weng, Y.; Chittaboina, S.; Zhuo, R.; Harrell, P. M.; Trinh, Y. T.; Zhang, Q.; Urbatsch, I. L.; Chang, G. Structure of P-glycoprotein reveals a molecular basis for poly-specific drug binding. *Science* **2009**, *323*, 1718−1722.

(10) Dantzig, A. H.; de Alwis, D. P.; Burgess, M. Considerations in the design and development of transport inhibitors as adjuncts to drug therapy. *Adv. Drug Delivery Rev.* **2003**, *55*, 133−150.

(11) Sandor, V.; Fojo, T.; Bates, S. E. Future perspectives for the development of P-glycoprotein modulators. *Drug Resist. Updates* **1998**, *1*, 190−200.

(12) Mahon, F. X.; Deininger, M. W. N.; Schultheis, B.; Chabrol, J.; Reiffers, J.; Goldman, J. M.; Melo, J. V. Selection and characterization of BCR-ABL positive cell lines with differential sensitivity to the tyrosine kinase inhibitor STI571: diverse mechanisms of resistance. *Blood* **2000**, *96*, 1070−1079.

(13) Eckford, P. D. W.; Sharom, F. J. ABC efflux pump-based resistance to chemotherapy drugs. *Chem. Rev.* **2009**, *109*, 2989−3011.

(14) Raub, T. J. P-Glycoprotein recognition of substrates and circumvention through rational drug design. *Mol. Pharmaceutics* **2006**, *3*, 3−25.

(15) Cole, S. P.C.; Bhardwaj, G.; Gerlach, J. H.; Mackie, J. E.; Grant, C. E.; Almquist, K. C.; Stewart, A. J.; Kurz, E. U.; Duncan, A. M.; Deeley, R. G. Overexpression of a transporter gene in a multidrug-resistant human lung cancer cell line. *Science* **1992**, *258*, 1650−1654.

(16) Slot, A. J.; Molinski, S. V.; Cole, S. P. C. Mammalian multidrug resistance proteins (MRPs). *Essays Biochem.* **2011**, *50*, 197−207.

(17) Deeley, R. G.; Westlake, C.; Cole, S. P. C. Transmembrane transport of endo- and xenobiotics by membrane ATP-binding cassette multidrug resistance proteins. *Physiol. Rev.* **2006**, *86*, 849−899.

(18) Rosenberg, M. F.; Mao, Q. C.; Holzenburg, A.; Ford, R. C.; Deeley, R. G.; Cole, S. P.C. The structure of the multidrug resistance protein (MRP1/ABCC1). Crystallization and single particle analysis. *J. Biol. Chem.* **2001**, *276*, 16076−16082.

(19) Loo, T. W.; Clarke, D. M. Covalent modification of P-glycoprotein mutants containing a single cysteine in either nucleotide-binding fold abolishes drug-stimulated ATPase activity. *J. Biol. Chem.* **1995**, *270*, 22957−22961.

(20) Urbatsch, I. L.; Sankaran, B.; Bhagat, S.; Senior, A. E. Both P-glycoprotein nucleotide-binding sites are catalytically active. *J. Biol. Chem.* **1995**, *270*, 26956−26961.

(21) Nagata, K.; Nishitani, M.; Matsuo, M.; Kioka, N.; Amachi, T.; Ueda, K. Nonequivalent nucleotide trapping in the two nucleotide binding folds of the human multidrug resistance protein MRP1. *J. Biol. Chem.* **2000**, *275*, 17626−17630.

(22) de Jong, M. C.; Slootstra, J. W.; Scheffer, G. L.; Schroeijers, A. B.; Puijk, W. C.; Dinkelberg, R.; Icool, M.; Broxterman, H. J.; Meloen, R. H.; Scheper, R. J. Peptide transport by the multidrug resistance protein MRP1. *Cancer Res.* **2001**, *61*, 2552−2557.

(23) Tombline, G.; Donnelly, D. J.; Holt, J. J.; You, Y.; Ye, M.; Gannon, M. K.; Nygren, C. L.; Detty, M. R. Stimulation of P-glycoprotein ATPase by analogues of tetramethylrosamine: coupling of drug binding at the "R" site to the ATP hydrolysis transition state. *Biochemistry* **2006**, *45*, 8034−8047.

(24) Tombline, G.; Holt, J. J.; Gannon, M. K.; Donnelly, D. J.; Wetzel, B.; Sawada, G. A.; Raub, T. J.; Detty, M. R. ATP occlusion by P-glycoprotein as a surrogate measure of drug coupling. *Biochemistry* **2008**, *47*, 3294−3307.

(25) Gannon, M. K.; Holt, J. J.; Bennett, S. M.; Wetzel, B. R.; Loo, T. W.; Bartlett, M. C.; Clarke, D. M.; Sawada, G. A.; Higgins, J. W.; Tombline, G.; Raub, T. J.; Detty, M. R. Rhodamine inhibitors of P-glycoprotein: an amide thioamide "switch" for ATPase activity. *J. Med. Chem.* **2009**, *52*, 3328−3341.

(26) Sawada, G. A.; Raub, T. J.; Higgins, J. W.; Brennan, N. K.; Moore, T. M.; Tombline, G.; Detty, M. R. Chalcogenopyrylium dyes as inhibitors/modulators of P-glycoprotein in multidrug-resistant cells. *Bioorg. Med. Chem.* **2008**, *16*, 9745−9756.

(27) Detty, M. R.; Gibson, S. L.; Wagner, S. Current clinical and preclinical photosensitizers for use in photodynamic therapy. *J. Med. Chem.* **2004**, *47*, 3897−3915.

(28) Gibson, S. L.; Holt, J. J.; Ye, M.; Donnelly, D. J.; Ohulchanskyy, T. Y.; You, Y.; Detty, M. R. Structure–activity studies of uptake and phototoxicity with heavy-chalcogen analogues of tetramethylrosamine

in vitro in chemosensitive and multidrug-resistant cells. *Bioorg. Med. Chem.* **2005**, *13*, 6394−6403.

(29) Holt, J. J.; Gannon, M. K.; Tombline, G.; McCarty, T. A.; Page, P. M.; Bright, F. V.; Detty, M. R. A cationic chalcogenoxanthylium photosensitizer effective in vitro in chemosensitive and multidrug-resistant cells. *Bioorg. Med. Chem.* **2006**, *14*, 8635−8643.

(30) McKnight, R. E.; Ye, M.; Ohulchanskyy, T. Y.; Sahabi, S.; Wetzel, B. R.; Wagner, S. J.; Skripchenko, A.; Detty, M. R. Synthesis of analogues of a flexible thiopyrylium photosensitizer for purging blood-borne pathogens and binding mode and affinity studies of their complexes with DNA. *Bioorg. Med. Chem.* **2007**, *15*, 4406−4418.

(31) Ohulchanskyy, T. Y.; Gannon, M. K., II; Ye, M.; Wagner, S. J.; Skripchenko, A.; Prasad, P. N.; Detty, M. R. Switched-on" flexible chalcogenopyrylium photosensitizers upon binding to DNA. Purging of viral pathogens through singlet-oxygen induced DNA cleavage. *J. Phys. Chem. B* **2007**, *111*, 9686−9692.

(32) Detty, M. R.; Merkel, P. B.; Hilf, R.; Gibson, S. L.; Powers, S. K. Chalcogenapyrylium dyes as potential photochemotherapeutic agents. II. Mitochondrial targeting and inhibition of cytochrome c oxidase in isolated mitochondrial suspensions. *J. Med. Chem.* **1990**, *33*, 1108−1116.

(33) Simard, T. P.; Yu, J. H.; Zebrowski-Young, J. M.; Haley, N. F.; Detty, M. R. Soluble infrared-absorbing croconate dyes from 2,6-di-*tert*-butyl-4-methylchalcogenopyrylium salts. *J. Org. Chem.* **2000**, *65*, 2236−2238.

(34) Sun, X.; Wong, J. R.; Song, K.; Hu, J.; Garlid, K. D.; Chen, L. B. AA1, A newly synthesized lipophilic cation, expresses potent in vivo antitumor activity. *Cancer Res.* **1994**, *54*, 1465−1471.

(35) Brennan., N. K.; Hall, J. P.; Davies, S. R.; Gollnick, S. O.; Oseroff, A. R.; Gibson, S. L.; Hilf, R.; Detty, M. R. In vitro photodynamic properties of chalcogenopyrylium analogues of the thiopyrylium antitumor agent AA1. *J. Med. Chem.* **2002**, *45*, 5123−5135.

(36) Leonard, K.; Nelen, M.; Raghu, M.; Detty, M. R. Chalcogenopyranones from disodium chalcogenide additions to 1,4-pentadiyn-3-ones. The role of enol ethers as intermediates. *J. Heterocycl. Chem.* **1999**, *36*, 707−717.

(37) Gannon, M. K., II; Detty, M. R. Generation of 3- and 5-lithiothiophene-2-carboxylates via metal−halogen exchange and their addition reactions to chalcogenoxanthones. *J. Org. Chem.* **2007**, *72*, 2647−2650.

(38) Parnham, W. E.; Sayed, Y. A. Synthesis of benzoylbenzoic acids. *J. Org. Chem.* **1974**, *39*, 2051−2053.

(39) Beak, P.; Brown, R. A. The *tertiary* amide as an effective director of *ortho* lithiation. *J. Org. Chem.* **1982**, *47*, 34−46.

(40) Leonard, K. A.; Nelen, M. I.; Anderson, L. T.; Gibson, S. L.; Hilf, R.; Detty, M. R. 2,4,6-Triarylchalcogenopyrylium dyes related in structure to the antitumor agent AA1 as in vitro sensitizers for the photodynamic therapy of cancer. *J. Med. Chem.* **1999**, *42*, 3942−3952.

(41) Sangster, J. In *Octanol−Water Partition Coefficients: Fundamentals and Physical Chemistry*; Wiley Series in Solution Chemistry; Fogg, P. G. T., Ed.; John Wiley and Sons: New York, 1997.

(42) Loe, D. W.; Almquist, K. C.; Deeley, R. G.; Cole, S. P. C. Multidrug resistance protein (MRP)-mediated transport of leukotriene C$_4$ and chemotherapeutic agents in membrane vesicles. Demonstration of glutathione-dependent vincristine transport. *J. Biol. Chem.* **1996**, *271*, 9675−9682.

(43) Ito, K.; Olsen, S. L.; Qiu, W.; Deeley, R. G.; Cole, S. P. C. Mutation of a single conserved tryptophan in multidrug resistance protein 1 (MRP1/ABCC1) results in loss of drug resistance and selective loss of organic anion transport. *J. Biol. Chem.* **2001**, *276*, 15616−15624.

(44) Shapiro, A. B.; Ling, V. Stoichiometry of rhodamine 123 transport to ATP hydrolysis by P-glycoprotein. *Eur. J. Biochem.* **1998**, *254*, 189−193.

(45) Loo, T. W.; Clarke, D. M Functional consequences of proline mutations in the predicted transmembrane domain of P-glycoprotein. *J. Biol. Chem.* **1993**, *268*, 3143−3149.

(46) Loo, T. W.; Clarke, D. M. Rapid purification of human P-glycoprotein mutants expressed transiently in HEK-293 cells by nickel-chelate chromatography and characterization of their drug-stimulated ATPase activities. *J. Biol. Chem.* **1995**, *270*, 21449−21452.

(47) Chifflet, S.; Torriglia, A.; Chiesa, R.; Tolosa, S. A method for the determination of inorganic-phosphate in the presence of labile organic phosphate and high-concentrations of protein—application to LENS ATPases. *Anal. Biochem.* **1988**, *168*, 1−4.

(48) Loo, T. W.; Clarke, D. M. Identification of residues in the drug-binding domain of human P-glycoprotein—analysis of transmembrane segment 11 by cysteine-scanning mutagenesis and inhibition by dibromobimane. *J. Biol. Chem.* **1999**, *274*, 35388−35392.

(49) Tsuruo, T.; Iida, H.; Tsukagoshi, S.; Sakurai, Y. Overcoming of vincristine resistance in P388 leukemia in vivo and in vitro through enhanced cytotoxicity of vincristine and vinblastine by verapamil. *Cancer Res.* **1981**, *41*, 1967−1972.

(50) Evers, R.; Kool, M.; Smith, A. J.; van Deemter, L.; de Haas, M.; Borst, P. Inhibitory effect of the reversal agents V-104, GF120918 and Pluronic L61 on MDR1P-gp-, MRP1- and MRP2-mediated transport. *Br. J. Cancer* **2000**, *83*, 366−374.

(51) Dantzig, A. H.; Shepard, R. L.; Law, K. L.; Tabas, L.; Pratt, S.; Gillespie, J. S.; Binkley, S. N.; Kuhfeld, M. T.; Starling, J. J.; Wrighton, S. A. Selectivity of the multidrug resistance modulator, LY335979, for P-glycoprotein and effect on cytochrome P450 activities. *J. Pharm. Exp. Ther.* **1999**, *290*, 854−890.

(52) Troutman, M. D.; Thakker, D. R. Rhodamine 123 requires carrier-mediated influx for its activity as a P-glycoprotein substrate in Caco-2 Cells. *Pharm. Res.* **2003**, *20*, 1192−1199.

(53) Sawada, G. A.; Barsuhn, C. L.; Lutzke, B. S.; Houghton, M. E.; Padbury, G. E.; Ho, N. F. H.; Raub, T. J. Increased lipophilicity and subsequent cell partitioning decrease passive transcellular diffusion of novel, highly lipophilic antioxidants. *J. Pharm. Exp. Ther.* **1999**, *288*, 1317−1326.

(54) Juvale, K.; Pape, V. F. S.; Wiese, M. Investigation of chalcones and benzochalcones as inhibitors of breast cancer resistance protein. *Bioorg. Med. Chem.* **2012**, *20*, 346−355.

(55) Pick, A.; Mueller, H.; Mayer, R.; Haenisch, B.; Pajeva, I. K.; Weigt, M.; Boenisch, H.; Mueller, C. E.; Wiese, M. Structure−activity relationships of flavonoids as inhibitors of breast cancer resistance protein (BCRP). *Bioorg. Med. Chem.* **2011**, *19*, 2090−2102.

(56) Haimeur, A.; Conseil, G.; Deeley, R. G.; Cole, S. P. C. The MRP-related and BCRP/ABCG2 multidrug resistance proteins: biology, substrate specificity and regulation. *Curr. Drug Metab.* **2004**, *5*, 21−53.

(57) Haecker, H.-G.; Leyers, S.; Wiendlocha, J.; Guetschow, M.; Wiese, M. Aromatic 2-(thio)ureidocarboxylic acids as a new family of modulators of multidrug resistance-associated protein 1: synthesis, biological evaluation, and structure−activity relationships. *J. Med. Chem.* **2009**, *52*, 4586−4595.

(58) Maeno, K.; Nakajima, A.; Conseil, G.; Rothnie, A.; Deeley, R. G.; Cole, S. P. C. Molecular basis for reduced estrone sulfate transport and altered modulator sensitivity of TM6 and TM17 mutants of MRP1 (*ABCC1*). *Drug Metab. Dispos.* **2009**, *37*, 1411−1412.

(59) Loo, T. W.; Bartlett, M. C.; Clarke, D. M. Methanethiosulfonate derivatives of rhodamine and verapamil activate human P-glycoprotein at different sites. *J. Biol. Chem.* **2003**, *278*, 50136−50141.

(60) Loo, T. W.; Clarke, D. M. Location of the rhodamine-binding site in the human multidrug resistance P-glycoprotein. *J. Biol. Chem.* **2002**, *277*, 44332−44338.

(61) Loo, T. W.; Bartlett, M. C.; Clarke, D. M. Substrate-induced conformational changes in the transmembrane segments of human P-glycoprotein. Direct evidence for the substrate-induced fit mechanism for drug binding. *J. Biol. Chem.* **2003**, *278*, 13603−13606.

(62) Hipfner, D. R.; Almquist, K. C.; Stride, B. D.; Deeley, R. G.; Cole, S. P. C. Location of a protease-hypersensitive region in the multidrug resistance protein (MRP) by mapping of the epitope of MRP-specific monoclonal antibody QCRL-1. *Cancer Res.* **1996**, *56*, 3307−3314.

(63) Hipfner, D. R.; Gauldie, S. D.; Deeley, R. G.; Cole, S. P. C. Detection of the Mr 190,000 multidrug resistance protein, MRP, with monoclonal antibodies. *Cancer Res.* **1994**, *5*, 5788−5792.

(64) Loe, D. W.; Almquist, K. C.; Deeley, R. G.; Cole, S. P. C. Multidrug resistance protein (MRP)-mediated transport of leukotriene C$_4$ and chemotherapeutic agents in membrane vesicles. Demonstration of glutathione-dependent vincristine transport. *J. Biol. Chem.* **1996**, *271*, 9675−9682.

(65) Létourneau, I. J.; Slot, A. J.; Deeley, R. G.; Cole, S. P. C. Mutational analysis of a highly conserved proline residue in MRP1, MRP2, and MRP3 reveals a partially conserved function. *Drug Metab. Dispos.* **2007**, *35*, 1372−1379.

(66) Loo, T. W.; Bartlett, M. C.; Clarke, D. M. Rescue of ΔF508 and other misprocessed CFTR mutants by a novel quinazoline compound. *Mol. Pharmaceutics* **2005**, *2*, 407−413.

(67) Loo, T. W.; Clarke, D. M. P-glycoprotein—associations between domains and molecular chaperones. *J. Biol. Chem.* **1995**, *270*, 21839−21844.